Physical and Biochemical Properties of Canine Knee Articular Cartilage Are Affected by Selected Surgical Procedures

by

Cynthia R. Lee

B.S. Bioengineering (1997)
University of California, Berkeley

Submitted to the Department of Mechanical Engineering
in Partial Fulfillment of the Requirements for the Degree of
Master of Science in Mechanical Engineering

at the

Massachusetts Institute of Technology

June 1999

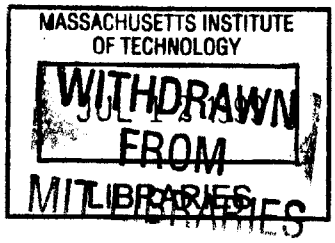

Signature of Author .....
Department of Mechanical Engineering
May 7, 1999

Certified by .....
Myron Spector
Senior Lecturer, Department of Mechanical Engineering
Professor of Orthopaedic Surgery (Biomaterials), Harvard Medical School
Thesis Supervisor

Accepted by .....
Ain A. Sonin
Chairman, Department Committee on Graduate Students

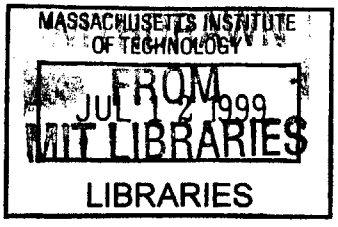

ENG

Physical and Biochemical Properties of Canine Knee Articular Cartilage are Affected by Selected Surgical Procedures

by

Cynthia R. Lee

Submitted to the Department of Mechanical Engineering on May 7, 1999
in Partial Fulfillment of the Requirements for the Degree of Master of Science
in Mechanical Engineering

ABSTRACT

The incomplete healing of articular cartilage defects is a common orthopaedic problem. Articular cartilage does not heal spontaneously and untreated lesions may progress to osteoarthritic degeneration. Consequently, a number of clinicians and researchers are committed to developing new methods to induce healing of chondral defects. With the emphasis on the effects of treatments on the cartilage defect, potential changes in the surrounding tissue have not yet been addressed.

This study utilizes a canine model to quantify changes that occur in articular cartilage fifteen to eighteen weeks after a knee joint is subjected to surgical treatment of isolated chondral defects. Clinical and experimental treatment of articular cartilage defects may include implantation of matrix materials and/or cells. The techniques evaluated here include four methods involved in the treatment of articular cartilage defects (microfracture, microfracture plus implantation of a type II collagen matrix, implantation of an autologous chondrocyte-seeded collagen matrix, and the harvest of trochlear ridge articular cartilage to obtain cells for the cell-seeded procedure).

Physical properties (thickness, equilibrium compressive modulus, dynamic compressive stiffness, and streaming potential) and biochemical composition (hydration, GAG content, DNA content) of the cartilage from various sites in these joints were compared to values measured for site-matched controls in unoperated knee joints. A number of significant changes were noted, with the patellar groove sites in the harvest-operated knees displaying up to three-fold increases in cartilage dynamic stiffness and streaming potential.

It is unknown whether or not the changes reported here will lead to osteoarthritic degeneration, but this study provides evidence that surgical treatment of chondral defects may elicit changes in the articular cartilage distant to the site being treated. Furthermore, treatment protocols that induce further trauma to the joint surface may lead to more severe changes.

Thesis Supervisor: Myron Spector
Title: Senior Lecturer, Department of Mechanical Engineering
Professor of Orthopaedic Surgery (Biomaterials), Harvard Medical School

ACKNOWLEDGEMENTS

I would like to thank everyone who has helped me complete this thesis. There are a few special people to whom I am especially grateful.

First, I must extend my gratitude to my advisor, Professor Spector, for all of his advice, encouragement, and enthusiasm.

Thank you to the Continuum Electromechanics Lab for accepting me as a member of your group. Thank you to Professor Grodzinsky for allowing me to use his facilities and for his advice and support of this project. Thank you to Eliot Frank who taught me the ins and outs of the Dynastat. Thank you to Steve Treppo for additional assistance with the intricacies of the Dynastat, for teaching me all of the biochemical assays, and for writing a great program (proAssay) to analyze all the biochemical data. Thank you to Marc Levenston and Andy Loening for showing me how to cut up joints. Additional thanks to Andy Loening who made me feel at home at my desk in 38-377 through his advice (solicited and otherwise) and entertaining antics. Thank you to Han-Hwa Hung for all her help with anything and everything.

Thank you to everyone in the Orthopaedic Research Lab at the Brigham and Women's Hospital. Special thanks to Sandra Taylor, who taught me everything I know about histology and who helped me embed and slice all the specimens; to Howie Breinan, Hu-Ping Hsu, and Scott Martin, who started the dog study before I came to MIT and let me use their animals for my research.

Thank you to the gang in 3-333 (Lila Chamberlain, Mark Spilker, Toby Freyman, and Stacy Morris) for all their advice on grad school and MIT.

Lastly, I would like to acknowledge the Whitaker Foundation and the Biokinetics Foundation for providing the financial support of this project.

TABLE OF CONTENTS

TABLE OF FIGURES AND TABLES

FIGURES

TABLES

CHAPTER 1: INTRODUCTION

1.1. Purpose of Research

Focal lesions in articular cartilage may arise from traumatic injury or disease. Healing of such lesions in adults is very limited and over time, the focal lesions may progress to osteoarthritis. In an effort to minimize the patient's risk for developing osteoarthritis, surgeons have developed a number of surgical techniques aimed at repairing articular cartilage defects (Minas and Nehrer, 1997). While the current procedures may achieve the goals of relieving pain and restoring function for many patients, they fail to provide full regeneration of articular cartilage. These procedures range from minimally invasive arthroscopic procedures to complex, open-joint operations. As scientists and clinicians continue to search for more effective methods for treating articular cartilage defects, the effects that different treatments have on the rest of joint becomes a compelling issue.

This thesis evaluates the effects of four different surgical procedures, developed to repair articular cartilage defects, on the articular cartilage throughout the rest of the joint. By quantifying changes in mechanical and biochemical properties induced by the four surgical procedures, this thesis also aims to determine if certain procedures may have the potential to be more detrimental to the joint than others.

1.2. Background

Articular cartilage is the aneural, avascular hyaline cartilage layer covering the bone ends at the articulating surface of diarthroidal joints. Chondrocytes are the specialized cells that are responsible for maintaining the cartilage matrix. In skeletally mature animals, chondrocytes are sparsely distributed throughout the matrix (roughly 10,000 cells/mm^3 in adult human femoral head cartilage; Venn and Maroudas, 1977) and are characterized by low mitotic activity.

Healthy articular cartilage functions to: 1) protect bones from abrasion and damage, 2) transmit and distribute high compressive loads to the bone, 3) provide joint congruity and maintain low contact stresses, and 4) provide a smooth, lubricated surface for joint articulation. The articular cartilage matrix that serves these functions is composed predominantly of water (65-75% of the total weight), type II collagen (50-90% of the dry weight) and charged proteoglycans (5-10% of the dry weight).

1.2.1 Mechanical Properties of Articular Cartilage

The low hydraulic permeability and high swelling tendency of the proteoglycan-rich network coupled with the tensile resistance of the collagen network give rise to the characteristic mechanical properties of articular cartilage, in particular the high compressive modulus and streaming potential. During compression, the swelling pressure, created by charge repulsion of the ionized proteoglycan molecules, resists deformation of articular cartilage. Deformation is further resisted by the tensile strength of the collagen fibers. Changes in either the collagen organization or proteoglycan content are reflected in changes in the compressive modulus of the tissue (Guilak *et al.*, 1994; Hoch *et al.*, 1983).

As articular cartilage is deformed, the mechanical pressure forces water out of the matrix. This time-dependent fluid exudation through the fixed charge network gives rise to an electric streaming potential. The magnitude of the streaming potential in response to dynamic compression is a sensitive measure of cartilage integrity and can detect changes in the tissue before changes are seen histologically or by standard mechanical tests (Bonassar *et al.*, 1995; Hoch *et al.*, 1983).

1.2.2 Natural Healing of Articular Cartilage

The avascularity and relative acellularity of adult articular cartilage results in a very limited capacity for natural repair. Partial thickness defects (*ie:* those restricted to the cartilage layer), in which no blood enters the wound, do not undergo any repair and may remain empty indefinitely (Mankin, 1982). Full-thickness defects that violate the subchondral bone can become partially filled with repair tissue (Mankin, 1982; Minas *et al.*, 1997) arising from the blood, marrow, and bone cells infiltrating the defect from the underlying, vascularized osseous tissue. The repair tissue, however, tends to be fibrous or fibrocartilaginous tissue, consisting predominately of type I instead of type II collagen. Although there may be some maturation of the repair tissue towards hyaline cartilage, maturation is incomplete and the repair tissue eventually begins to deteriorate (Minas *et al.*, 1997).

1.2.3 Factors Affecting Cartilage Degradation

It is unclear which factors lead to degradation of articular cartilage. Enzymes, such as collagenases and aggrecanases, and regulators, such as IL-1, TNF-α, and various metalloproteinases, can all contribute to the breakdown of the articular cartilage matrix (Dodge and Poole, 1989; Imai *et al.*, 1997; Lohmander *et al.*, 1993; Pettipher *et al.*, 1986; Testa *et al.*, 1994; Webb *et al.*, 1997). These enzymes and regulators appear to be released from chondrocytes and synovial membrane cells. For example, IL-1 is released by the cells in the synovial membrane as part of an inflammatory response and has been linked to the loss of matrix proteoglycans (Bird *et al.*, 1997; Pettipher *et al.*, 1986).

Normal articular cartilage function depends on the low hydraulic permeability and the hydrophilic nature of the proteoglycans and the tensile strength of the collagen fiber network (Poole, 1992). Thus, changes in proteoglycan and/or collagen content will lead to altered loading of the articular cartilage and underlying bone. Altered loading may further lead to erosion and degradative changes in the cartilage, due to the metabolic response of chondrocytes to changes in mechanical loads and the positive feedback to the cells responsible for the initial release of enzymes and regulators (Poole, 1992).

1.2.4 Cartilage Repair Procedures

A number of surgical procedures have been developed and continue to be investigated with the aim of promoting healing of articular cartilage defects (Minas *et al.*, 1997). Procedures that are currently used by orthopaedic surgeons to treat cartilage defects range from arthroscopic procedures aimed at inducing bleeding from the subchondral bone (*ie:* abrasion arthroplasty, microfracture), to open procedures that involve implantation of cells (autologous cell implantation, ACI; Brittberg *et al.*, 1994) or bone-cartilage grafts (mosaicplasty).

More recently, tissue engineering approaches have been used to attempt regeneration of articular cartilage in various animal models. Tissue engineering may

involve natural or synthetic matrices, cells from various sources, and/or regulators (Lee and Spector, 1998). One matrix studied as a potential candidate for improving articular cartilage repair is a type II collagen-glycosaminoglycan porous sponge. This type of matrix, both cell-seeded and unseeded has been studied *in vitro* and *in vivo* in a canine model (Breinan, 1998; Nehrer *et al.*, 1997).

1.2.5 Potential Hazards of Cartilage Repair Procedures

The effects of the various cartilage repair procedures on the rest of the joint have not been studied. It has been documented that arthrotomy alone may induce changes in the articular cartilage, but the effects appear to be short-lived (Havdrup and Telhag, 1978; Havdrup and Telhag, 1980; Speer *et al.*, 1990). More invasive procedures may lead to more permanent effects by creating particulate debris, additional tissue damage and/or inducing an inflammatory response. For example, the microfracture technique causes trauma to the underlying subchondral bone and draws blood along with various cell types and chemical regulators into the joint. Furthermore, the harvest procedures that are necessary for ACI and mosaicplasty create new defects in previously healthy articular cartilage. For the ACI procedure, slices of articular cartilage are harvested from the patient's trochlear groove. Superficial defects, such as those created during this harvest procedure, are even less likely to heal than full-thickness defects (Mankin, 1982) and may even lead to osteoarthritic changes (Grande *et al.*, 1989).

The introduction of a foreign matrix into the defect site may further lead to changes in the surrounding articular cartilage. Potential problems arise from fixation of the implant into the defect, the body's response to the implanted material, and the effects of matrix degradation and the degradation by-products. For example, a common method of fixing the matrices in the defects involves suturing of a flap over the defect site. Breinan, et al, found that the suture tracts remained with no signs of healing one year post-operatively (Breinan *et al.*, 1997). Additionally, Messner and Gillquist reported that implantation of synthetic matrices into defects led to an increase in surface irregularities of articular cartilage throughout the treated joints (Messner and Gillquist, 1993).

1.3. Specific Aim and Hypotheses

The specific aim of this research was to determine how four specific surgical procedures associated with articular cartilage repair affect the physical, biochemical and histological properties of the articular cartilage distant to the affected sites. A canine model was used to study the effects of three aspects of tissue engineering, matrix implantation, cell implantation, and autologous cell harvest. The three repair procedures investigated in this study include a microfracture procedure as a control procedure that is used clinically; microfracture and implantation of a porous type II collagen sponge to study the effects of an analog extracellular matrix; and implantation of a type II collagen sponge seeded with cultured autologous chondrocytes to study the effects of implanted cells. Lastly, the effects of an associated articular cartilage harvest were studied to determine the magnitude of damage induced when obtaining autologous cells.

The working hypothesis is that selected surgical procedures result in alterations in the properties of articular cartilage throughout the joint. It is also hypothesized that more invasive treatments may lead to greater changes.

CHAPTER 2: MATERIALS AND METHODS

2.1. Experimental Measurements

2.1.1 Physical properties

Articular cartilage is a load-bearing tissue. As it degrades, the ability of the tissue to sustain and distribute loads decreases. To determine if the surgical procedures induced such degradative changes, the equilibrium and dynamic stiffness of the articular cartilage was measured at eight to ten sites in the joint. Dynamic stiffness was measured over a range of frequencies as high frequency measurements are more sensitive to superficial changes and lower frequency measurements reflect properties at deeper levels.

The water content of articular cartilage and the presence of charged proteoglycans lead to compression-induced streaming potentials. These streaming potentials have proven to be a sensitive indicator of cartilage degradation (Frank and Grodzinsky, 1987; Frank and Grodzinsky, 1987; Frank *et al.*, 1987) and were therefore measured at various frequencies. Similar to the frequency dependence of dynamic stiffness, the streaming potentials measured at high frequencies are reflective of the properties near the surface while lower frequency measurements are influenced by the bulk.

Lastly, the thickness of the articular cartilage was measured. The thickness of the articular cartilage can indicate tissue hypertrophy and degradation. Furthermore, the exact tissue thickness was necessary to calculate the applied strain imposed on the tissue.

2.1.2 Biochemical composition

Early signs of cartilage degradation include increased water content and cell necrosis (Bullough *et al.*, 1985). The cellular response to mild degradation includes mild increases in cellularity and increased synthesis of glycosaminoglycans (Bullough *et al.*, 1985). Thus, hydration, total GAG content, and DNA content were measured at seven different sites in the joint and the values for the four surgical groups were compared with site-matched the values measured for the unoperated control group.

2.1.3 Histology

The majority of previously published work on articular cartilage repair and degradation has focused on the histological characteristics of the tissue. Major criteria for grading degenerative articular cartilage are the concentration and distribution of charged proteoglycans (Mankin *et al.*, 1971). For this reason, articular cartilage was prepared for staining with Safranin-O so that meaningful changes in proteoglycan could be analyzed in a traditional manner (described in section 2.5.3).

It has recently been observed by other researchers in the laboratory (unpublished data) that chondrocytes in the vicinity of articular cartilage defects contain the actin isoform characteristic of smooth muscle cells and myofibroblasts (α-smooth muscle actin, α-SMA). The role of α-SMA containing chondrocytes is not clear. Nonetheless, in order to determine if chondrocytes distant to the defect also contained α-SMA, selected specimens were prepared for immunohistochemical staining.

2.2. Experimental Groups

2.2.1 Animals

Twelve adult (skeletally mature) hound dogs (25-30 kg) were used in this study. The animal experiment was approved by the Brockton/West Roxbury VA Animal Care Committee. Detailed descriptions of animal surgery and animal care are described elsewhere (Breinan *et al.*, 1997). Briefly, two 4-mm diameter defects down to the level of the calcified cartilage were made in the trochlear groove of the right knees of all twelve canines. Defects were then treated by one of three methods described below (section 2.2.2). The right knees of all dogs were immobilized by external fixation for ten days after surgery, after which the animals were allowed to ambulate freely. The animals appeared to ambulate normally following removal of the external fixation. There was no indication that the animals favored either hind limb.

2.2.2 Surgical Groups

The defects of eight of the dogs were subject to microfracture, a clinically used technique in which the calcified cartilage was lightly scraped and a small pick was used to puncture the subchondral bone and induce bleeding into the defect site. This was the only treatment given to four of these dogs (microfracture group, μfx; n=4 dogs). The other four dogs had porous type II collagen sponges (Chondrocell, Geistlich Biomaterials, Wolhusen, Switzerland) implanted into the microfracture treated defects (matrix group, n=4). The pore characteristics of the type II sponges have been described previously (Nehrer *et al.*, 1997). Type II collagen films were sutured over the defects to secure the matrix in the defect. The film was produced from the same slurry used to make the matrices and was cross-linked with ultraviolet radiation (Nehrer *et al.*, 1997). The defects in the remaining four dogs were treated with type II collagen sponges seeded with cultured autologous chondrocytes (cell-seeded group, n=4). Implants were again fixed in the defect by suturing a type II collagen film over the defect.

The chondrocytes used to seed the matrices in the cell-seeded group were obtained from cartilage harvested from the contralateral (left) knees and expanded in culture for three weeks prior to treatment of the defects. Cartilage was harvested from the trochlear ridges by removing a strip of tissue approximately 20-25 mm long and 3-5 mm wide, down to the tidemark. This procedure yielded 300-350 mg (wet weight) of tissue. The harvesting procedure was performed on five of the left knees (harvest group, n=5), with the cells from one of the joints not being used. The left knees of the seven remaining dogs were unoperated and served as controls (control group, n=7). It was not anticipated that there would be any differences in tissue properties or composition between right and left knees (Athanasiou *et al.*, 1991).

2.3. Specimen Procurement and Allocation

Animals were sacrificed fifteen weeks after treatment of the defects (eighteen weeks after the harvest procedure). Immediately after sacrifice, the knee joints were opened under sterile conditions and the defect and harvest sites removed with a coping saw for histomorphometric analysis (Breinan, 1998). The remaining portion of each joint was then wrapped in saline-soaked gauze and transported from the operating room to the laboratory.

Eight sites on the right knee and ten sites on the left knee (Figure 2.1) were identified for mechanical testing, yielding a total of 216 specimens. A custom made coring bit, 9.5-mm internal diameter, fixed to a standard drill press was used to obtain osteochondral cores from each identified site on the femur and from each tibial plateau. The shaft of each long bone was clamped in a jig which allowed the rotation of the bone so that the joint surface at each desired location could be positioned parallel to the cutting edge of the coring bit. The joint surface and coring bit were kept moist throughout the entire process with phosphate buffered saline (PBS). Prior to removal of the tibial cores, the two testing sites (central and posterior) on each tibial core were marked with India ink.

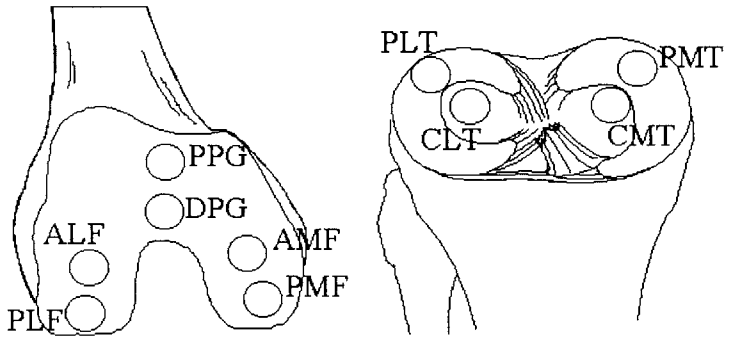

Figure 2.1 – Schematic illustration of femur (left) and tibia (right) showing sites identified for mechanical testing of articular cartilage. PLF=posterior lateral femoral condyle, ALF=anterior lateral femoral condyle, PPG=proximal patellar groove, DPG=distal patellar groove, AMF=anterior medial femoral condyle, PMF=posterior medial femoral condyle, CLT=central lateral tibial plateau, PLT=posterior lateral tibial plateau, PMT=posterior medial tibial plateau, CMT=central medial tibial plateau. PPG and DPG sites correspond to the defect sites in right knees which were removed for histomorphometric evaluation. PPG and DPG sites were only tested in harvest and control knee joints. All sites except DPG, PMF, and PLF sites were also analyzed for biochemical composition.

Osteochondral cores that were damaged during retrieval were discarded. The remaining cores were immersed in PBS and frozen at –20°C until the day of testing.

The articular cartilage and underlying bone surrounding the cores was placed in 10% neutral buffered formalin and processed for histological study.

2.4. Mechanical Testing

An indentation test protocol was employed, in part, in anticipation of future studies of the mechanical properties of reparative tissue that would not be suitable for confined compression testing. The indentation protocol was used to measure equilibrium stiffness, dynamic stiffness, and streaming potential. Additionally, a needle-ramp method was used to measure articular cartilage thickness.

2.4.1 Testing Setup

2.4.1.1. Dynastat Mechanical Spectrometer

A Dynastat mechanical spectrometer (IMASS, Hingham, MA) was used to perform mechanical testing. The Dynastat was connected to a computer that controlled displacement of the actuator and recorded the resulting loads and potentials.

2.4.1.2. Indenter

The indenter used in this study was a 1-mm plane-ended plexiglass indenter equipped with a 250-μm diameter Ag/AgCl electrode. The electrode was used to measure the compression-induced streaming potentials during sinusoidal compressions (Lin *et al.*, 1998).

2.4.1.3. Specimen Preparation

On the day of testing, osteochondral cores were thawed in phosphate buffered saline with 10mM EDTA serving as a general proteinase inhibitor (PBE). The thawed specimens were then mounted in self-curing polymethyl methacrylate (Quickmount, Fulton Metallurgical Products Corp., Saxonburg, PA). Care was taken to mount only the underlying bone in the Quickmount. Curing of the Quickmount took twenty to thirty minutes. To minimize fluid loss during this time, the cartilage surface was covered with tissue soaked in PBE. The mounted specimen was then placed in a plexiglass chamber with five rotational/translational degrees of freedom or stored in PBE at 4°C until testing was ready to commence. Specimens stored at 4°C were allowed to reach room temperature prior to testing.

The plexiglass chamber was fixed in the lower jaw of the Dynastat and adjusted so that the articular surface of the specimen was perpendicular to the axis of the indenter. The chamber was then filled with PBE and the tissue allowed to equilibrate for ten minutes and regain any fluid lost during the mounting and positioning process.

2.4.2 Stress Relaxation

Mechanical testing began with a tare load of approximately 0.01 kg to ensure complete contact between the indenter and the cartilage. The cartilage was allowed to relax under the tare load for five minutes.

To measure equilibrium behavior, stress relaxation tests at three different strain levels were performed. Using displacement control of the Dynastat, three ramp and hold displacements corresponding to approximately 10%, 15% and 20% strain (based on estimated tissue thickness) were applied. The total time to achieve the desired displacement was 180 seconds and the displacement was held for an additional 320 seconds. The load and displacement were continuously recorded. Load and displacement measurements were then converted to stress and strain, using the area of the indenter and the actual thickness of the tissue, as measured by the needle ramp method described below (section 2.4.5). A stress relaxation curve for a typical specimen is shown in Figure 2.2.

To determine the equilibrium compressive modulus, the equilibrium stress was first plotted versus strain. A first order polynomial was fit to the stress-strain data and the

slope of the line recorded. Using the analysis of Hayes, *et al.* (Hayes *et al.*, 1972), an effective equilibrium Young's modulus of the tissue was calculated from this slope, Poisson's ratio (ν), the aspect ratio (a/h; indenter radius/tissue thickness), and a tabulated parameter (κ, based on ν and a/h; Hayes *et al.*, 1972).

$$E = (\sigma/\varepsilon)(1-\nu^2)\pi(a/h)/2\kappa \quad (1)$$

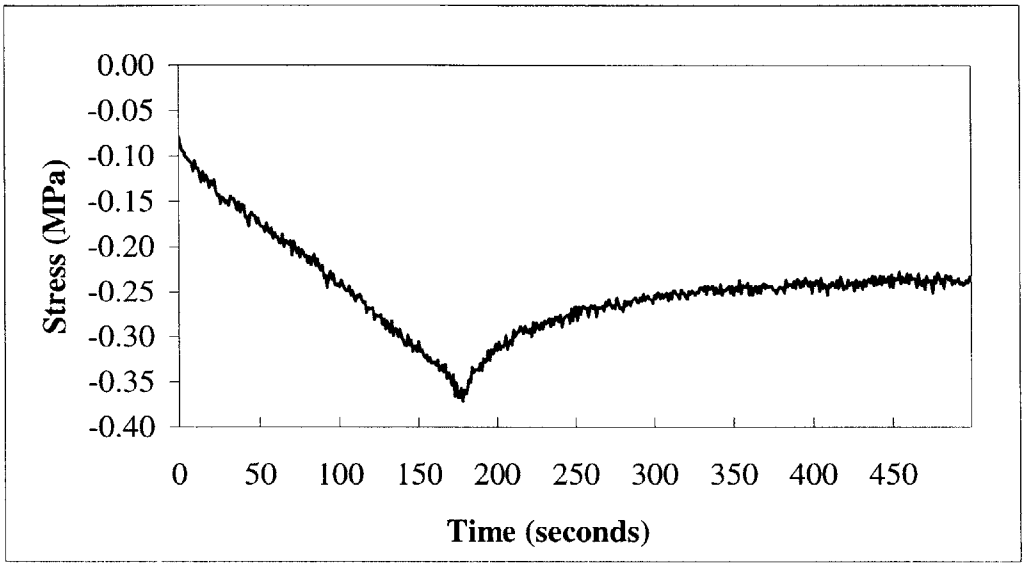

Figure 2.2 – Typical stress relaxation curve of articular cartilage during indentation ramp (0-180 seconds) and hold (180-500 seconds) displacement.

Poisson's ratio for articular cartilage varies by species and site. We used values reported for canine articular cartilage by Athanasiou (Athanasiou *et al.*, 1991) for the femoral sites and by Setton (Setton *et al.*, 1994) for the tibial sites. These values ranged from 0.05 for the tibial sites to 0.30 for the femoral condyles.

2.4.3 Dynamic Stiffness

Sinusoidal displacements with amplitudes of approximately 1% strain and frequencies of 1.0, 0.5, 0.1, 0.05, 0.01, and 0.005 Hz, were superimposed on the 15% static strain. The resulting loads and displacements were recorded and converted to stress and strain, respectively. Dynamic stiffness was then calculated as the ratio of stress to strain. To account for differences in material stiffening due to differences in the applied offset strain, as the tissue thickness was initially unknown, dynamic stiffness was normalized to the static offset stress.

2.4.4 Streaming Potential

The streaming potentials generated by the sinusoidal displacements were detected by the Ag/AgCl electrode in the probe and recorded by the computer. The potentials were measured relative to the potential of the PBE bath and reported as voltage divided

by dynamic strain amplitude. Again, to account for material stiffening, the streaming potentials were normalized to the static offset stress.

2.4.5 Thickness Measurements

After mechanical testing, the indenter was removed and a needle probe was clamped into the upper jaw of the Dynastat. A needle ramp method described by Hoch, *et al.* (Hoch *et al.*, 1983) was used to measure articular cartilage thickness at the site of indentation testing. As the needle contacted the upper surface of the hydrated tissue, an electrical circuit was completed, resulting in a step change in the voltage. When the needle reached the underlying calcified cartilage, there was a step increase in the load. These step changes were detected by computer analysis and the ramp rate and time between step changes were used to determine the articular cartilage thickness.

2.5. Biochemical Analysis

Biochemical analysis was performed on seven of the ten sites identified for mechanical testing. After mechanical testing and thickness measurements of these sites, a scalpel was used to remove full-thickness slices of articular cartilage from half of the plug. Care was taken to remove as much of the articular cartilage as possible without removing any of the calcified cartilage. The slices of cartilage were weighed (section 2.5.1) and frozen for later biochemical analysis.

The remaining articular cartilage and subchondral bone was placed in 10% neutral buffered formalin and processed for histology. For the three sites that were not subject to biochemical analysis (distal patellar groove, posterior medial and lateral femoral condyles), the entire plug was placed in formalin immediately after thickness measurements were completed.

2.5.1 Hydration

Excess water was dried from the slices of removed cartilage and the wet weight of the tissue measured. The slices of tissue were then frozen at –20°C. The frozen tissue was later lyophilized for thirty to forty hours and dry weights measured. Hydration was determined as follows:

$$\text{hydration} = (\text{wet weight} - \text{dry weight})/\text{dry weight} \qquad (2)$$

2.5.2 Glycosaminoglycan Content

Lyophilized tissue was digested in 1.5-4 mls of papain (1.76 mg/ml cysteine, 0.125 mg/ml papain in PBE) for at least twelve hours at 60°C. Papain digests of the tissue were analyzed for total glycosaminoglycan content using the DMMB dye binding assay. A spectrophotometer (Perkin-Elmer Lambda 3b) measured absorbance at 525 nm. Shark chondroitin-6-sulfate was used as the standard. Using the curve derived from the standards, absorbance measurements were converted to GAG content.

2.5.3 DNA Content

Papain digests were also analyzed for DNA content using Hoechst 33528 dye fluorescence. Fluorescence was measured on a spectrafluorometer (SPF-500c, SLM

Instruments). To account for autofluorescence of the digests, fluorometer readings were made both with and without Hoechst 33258 dye. Calf thymus DNA was used as the standard. The DNA content was interpolated from the fluorometer measurements and the standard curve.

2.6. Histology and Immunohistochemistry

Articular cartilage and underlying bone from areas around the tested cores were allocated for histology on the day of animal sacrifice. The articular cartilage and underlying bone from tested cores and not used for biochemical analysis was allocated for histology after mechanical testing.

2.6.1 Fixation and Decalcification

Tissue allocated for histology was fixed in 10% neutral buffered formalin for five to six days. After fixation, specimens were decalcified in 15% EDTA solution for at least 28 days.

2.6.2 Embedding and Sectioning

After fixation and decalcification, tissue was dehydrated through a series of alcohol baths. Tissue was then embedded in either glycol methacrylate (JB-4, Polysciences, Inc., Warrington, PA) or paraffin.

Select specimens were sectioned to five (JB-4 embedded specimens) or seven (paraffin embedded specimens) micrometers in thickness.

2.6.3 Light Microscope Analysis

JB-4 sections were stained with Safranin-O/Fast Green. The Mankin scale (Mankin *et al.*, 1971) was used to make a semi-quantitative assessment of the degradative changes of the tissue in the selected specimens. The Mankin scale grades cartilage degradation based on cellularity (0-3 points), distribution of proteoglycan staining (0-5), surface continuity (0-4), and integrity of the subchondral bone (0-1). The Mankin scale ranges from 0-14, with normal articular cartilage scoring zero.

Immunohistochemistry was used to stain paraffin sections for the contractile protein, α-smooth muscle actin, using a monoclonal antibody to the protein. Blood vessels in the subchondral bone were used as positive controls and sections treated with mouse serum instead of the monoclonal antibody served as the negative controls.

2.7. Statistical Analysis

2.7.1 Power Calculation of Sample Size

This study sought to identify changes in the mechanical and biochemical properties of the surrounding articular cartilage that could potentially have a clinically meaningful effect. That this was an initial investigation and conducted at a relatively early time point (15-18 weeks post-operatively), it was anticipated that a change of 50% would be compelling. Based on literature values for selected mechanical properties of canine articular cartilage, we estimated a standard deviation of 25%. For a desired power of 80% (β=0.20) and α=0.05, a sample size of four was required.

2.7.2 Statistical Analysis of Results

The measured properties at each site for each surgical group were compared to the average values measured at the same site in the unoperated control group. An unpaired Student's t-test assuming equal variances was performed on Excel. Statistical analysis was also performed using the Fisher Exact test. After counting the number of occurences of high and low values, the Fisher Exact test was performed using a program on the Internet (http://www.nr.no/~langsrud/fisher.htm). The criterion for significance was $p<0.05$, but changes with a p-value of less than 0.10 are also noted.

CHAPTER 3: RESULTS

3.1. Specimen Procurement

There was no indication that the animals favored either hind limb in the weeks following surgery. In previous studies involving surgery (*viz.*, total hip replacement) on the hind limbs of dogs, quantitative gait analysis and analyzed computed tomography of the tibias demonstrated that animals ambulating normally, as those in this study, applied equal load bearing on the hind limbs.

At necropsy, there was no evidence of joint inflammation or gross abnormalities in the articular cartilage distant from the defect and harvest sites. The defect and harvest sites were easily identified at necropsy. Histomorphometric evaluation of the tissue filling the original defects revealed predominately fibrocartilage in all of the defects (Breinan, 1998).

A total of nine specimens were lost during specimen retrieval, leaving a total of 207 specimens for mechanical testing.

3.2. Physical Properties

Significant changes ($p<0.05$ by Student's t-test and/or Fisher Exact test), ranging from 36 to 300% of control values were seen in the dynamic mechanical properties (Table 3.1). These changes were seen at three sites in the harvest (DPG, PPG, and CLT) and cell-seeded matrix (PLF, PMF, CLT) groups and at two sites in the matrix group (CLT and PLT). At the $p<0.10$ level, six of the ten sites in the harvest group, four of the eight sites in the cell-seeded matrix and microfracture groups, and three of the eight sites in the matrix group showed changes in at least one mechanical property. No changes ($p<0.10$) were seen in any treatment group at the CMT, ALF or AMF sites. All changes in physical properties with $p<0.10$ are shown as percent changes from the (unoperated) control values in Table 3.1.

3.2.1 Thickness

Articular cartilage thickness varied with site. Figure 3.1 shows how the mean cartilage thickness in the unoperated (control) joints varied from site to site. The range of values was from a low of 0.5 ± 0.05 mm (mean $\pm$ standard error of the mean) at the DPG site to a high of 1.4 ± 0.05 mm at the CMT.

Figure 3.2 shows how the articular cartilage thickness of the operated joints compared to the thickness of the unoperated control joints. There were no significant changes ($p<0.05$, by Student's t-test or Fisher Exact test) in cartilage thickness at any of the sites between any of the operated groups and the unoperated control group. However, there were a few sites where there were notable differences ($p<0.10$) between operated and unoperated groups (shown as percent changes in Table 3.1). The cartilage at the DPG increased from an average thickness of 0.47 ± 0.05 mm in the control group to 0.63 ± 0.03 mm in the harvest group, an increase of 33%. Other trends ($p_{Fisher}<0.10$) included decreases in tissue thickness at the PMF (thickness of control group 1.19 ± 0.07 mm) in the matrix (1.01 ± 0.18 mm) and microfracture (1.10 ± 0.09 mm) groups; at the CLT in

the matrix group (1.01 ± 0.12 mm versus 1.25 ± 0.10 mm for the control); and at the PMT in the microfracture group (0.81 ± 0.20 mm versus 0.99 ± 0.07 mm for control).

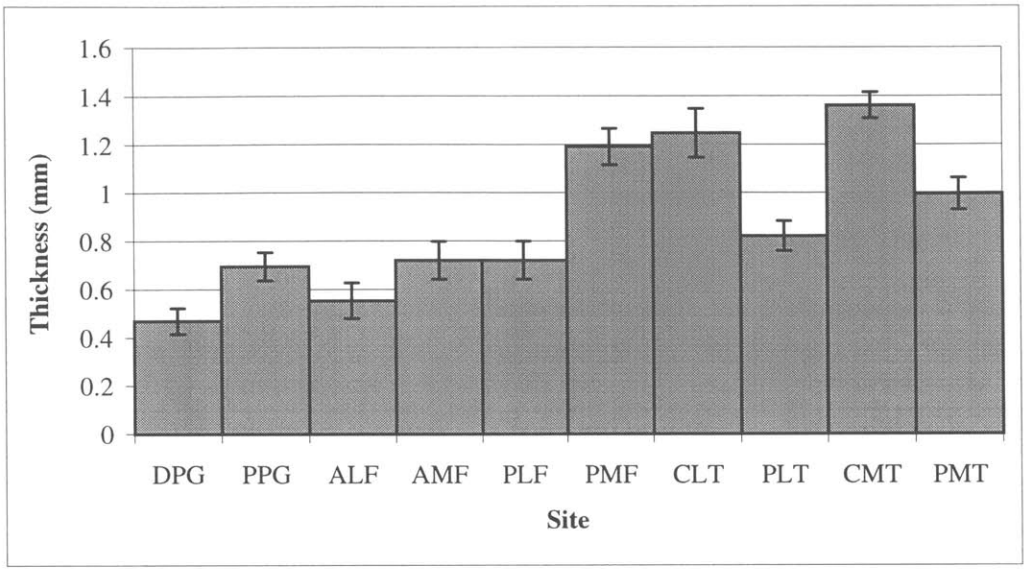

Figure 3.1 – Canine articular cartilage thickness at selected sites in unoperated joints. Values are mean ± SEM, n=6-7.

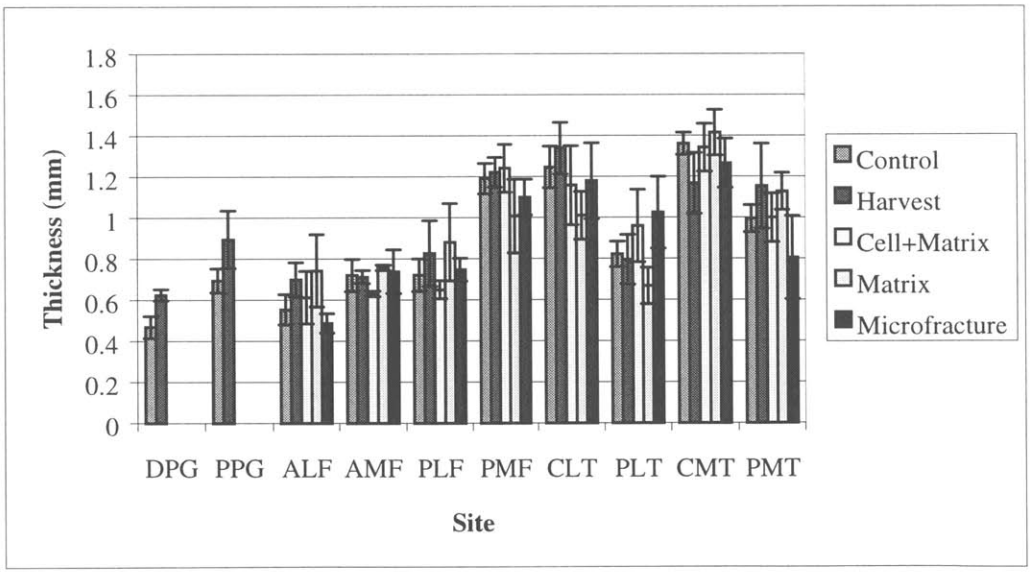

Figure 3.2 – Canine articular cartilage thickness at various sites in joints subjected to different surgical procedures. Values are mean ± SEM (n=3-7).

3.2.2 Equilibrium Modulus

The effective equilibrium Young's modulus also varied by site (Figure 3.3). The moduli for the unoperated joints ranged from 1.9 ± 0.1 MPa at the posterior lateral femoral condyle to 3.7 ± 0.7 MPa at the DPG.

Figure 3.4 shows how the equilibrium moduli for the different surgical groups compare. Again, there were no changes between operated and unoperated groups that reached a significance level of $p<0.05$ by the t-test. However, the modulus of the CLT was significantly higher, by 37 ± 24%, in the cell-seeded matrix group compared to the control group when analyzed with the Fisher exact test ($p=0.024$). At the $p<0.10$ level (Fisher test), the moduli also tended to increase at the CLT in the microfracture group. The moduli in the same three groups (harvest, cell-seeded matrix, and microfracture) tended to decrease at the PLF ($p<0.10$).

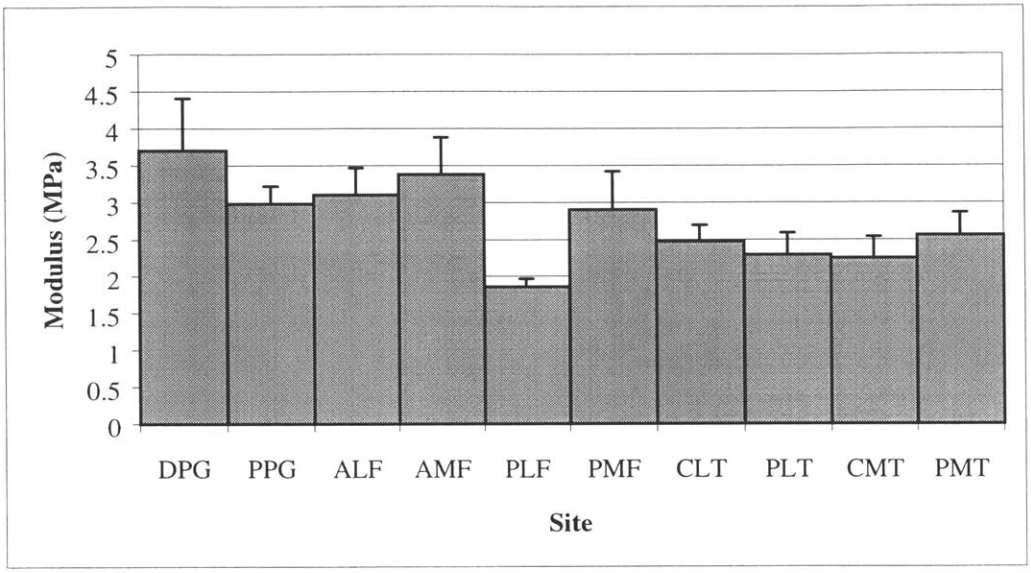

Figure 3.3 – Equilibrium compressive modulus of canine articular cartilage at selected sites in unoperated knee joints. Values are mean ± SEM, n=6-7.

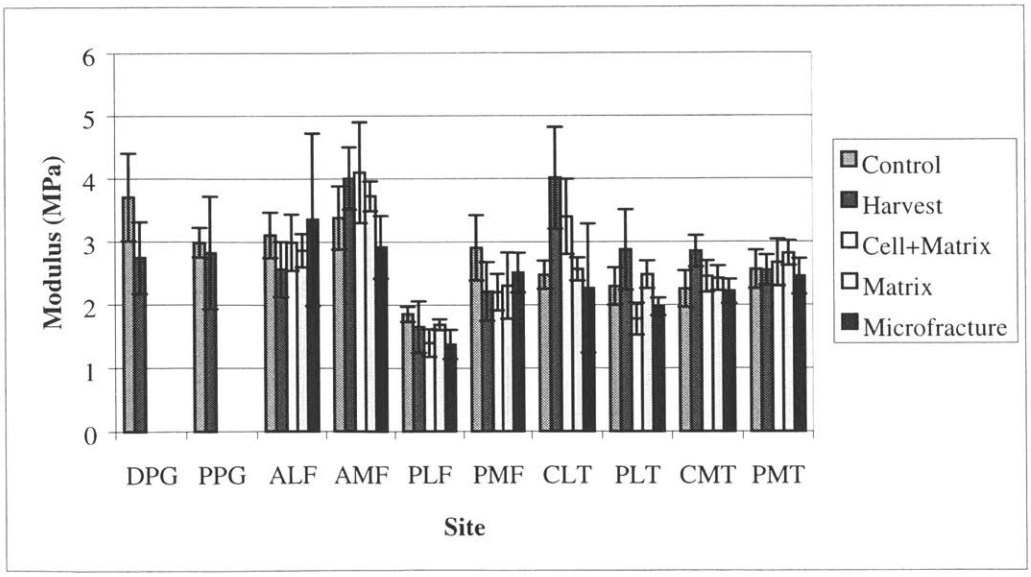

Figure 3.4 – Equilibrium compressive modulus of articular cartilage at various sites in joints subjected to different surgical procedures. Values are mean ± SEM (n=3-7).

3.2.3 Dynamic Stiffness

Dynamic stiffness was measured at six frequencies ranging from 0.005 to 1.0 Hz. As shown in Figure 3.5, dynamic stiffness typically increased with increasing frequency. The stiffness-frequency relationship illustrated in Figure 3.5 was similar for all sites and surgical treatments tested. Thus for the purpose of comparing the effects of different surgical treatments, the dynamic stiffnesses at 1.0 and 0.01 Hz for each specimen were analyzed. Preliminary analysis indicated that, in general, if differences were seen at one frequency, they were seen at all frequencies.

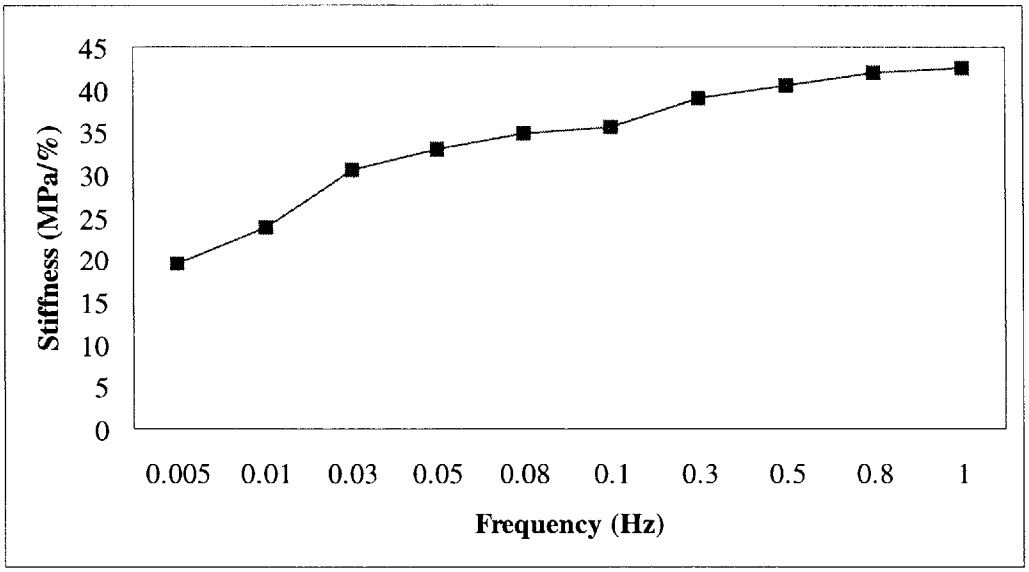

Figure 3.5 – Dynamic stiffness versus frequency of applied displacement for a canine articular cartilage at the distal patellar groove (DPG) site in an unoperated knee.

The range of dynamic stiffness normalized to static offset stress seen in the unoperated joints at 0.01 Hz (Figure 3.6a) was 22.4 ± 2.1 MPa/MPa (CMT) to 44.3 ± 3.5 MPa/MPa (PLF). At 1.0 Hz (Figure 3.6b), dynamic stiffness was again lowest at the CMT (35.2 ± 3.9 MPa/MPa) and the highest dynamic stiffness at this frequency was at the ALF (98.6 ± 19.5 MPa/MPa).

As illustrated in Figure 3.7, the tendency was for dynamic stiffness to be higher in the operated groups versus the unoperated control. Differences in the dynamic stiffnesses (compared to control) are summarized in Table 3.1.

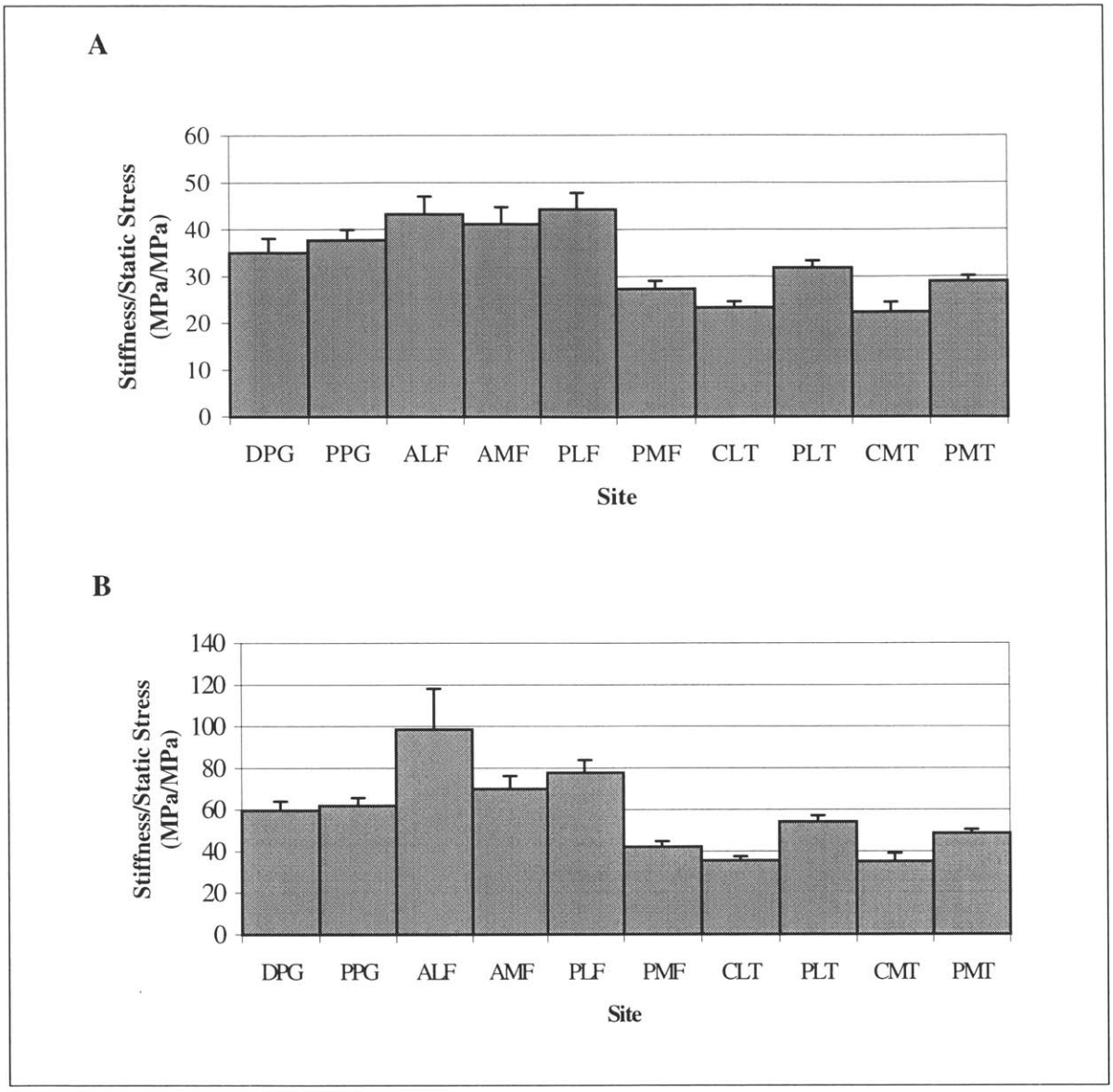

Figure 3.6 – Dynamic stiffness of canine articular cartilage at selected sites in unoperated knee joints (n=6-7) measured at **A:** 0.01 Hz and **B:** 1.0 Hz. Values are mean ± SEM and normalized to static offset stress; n=6-7.

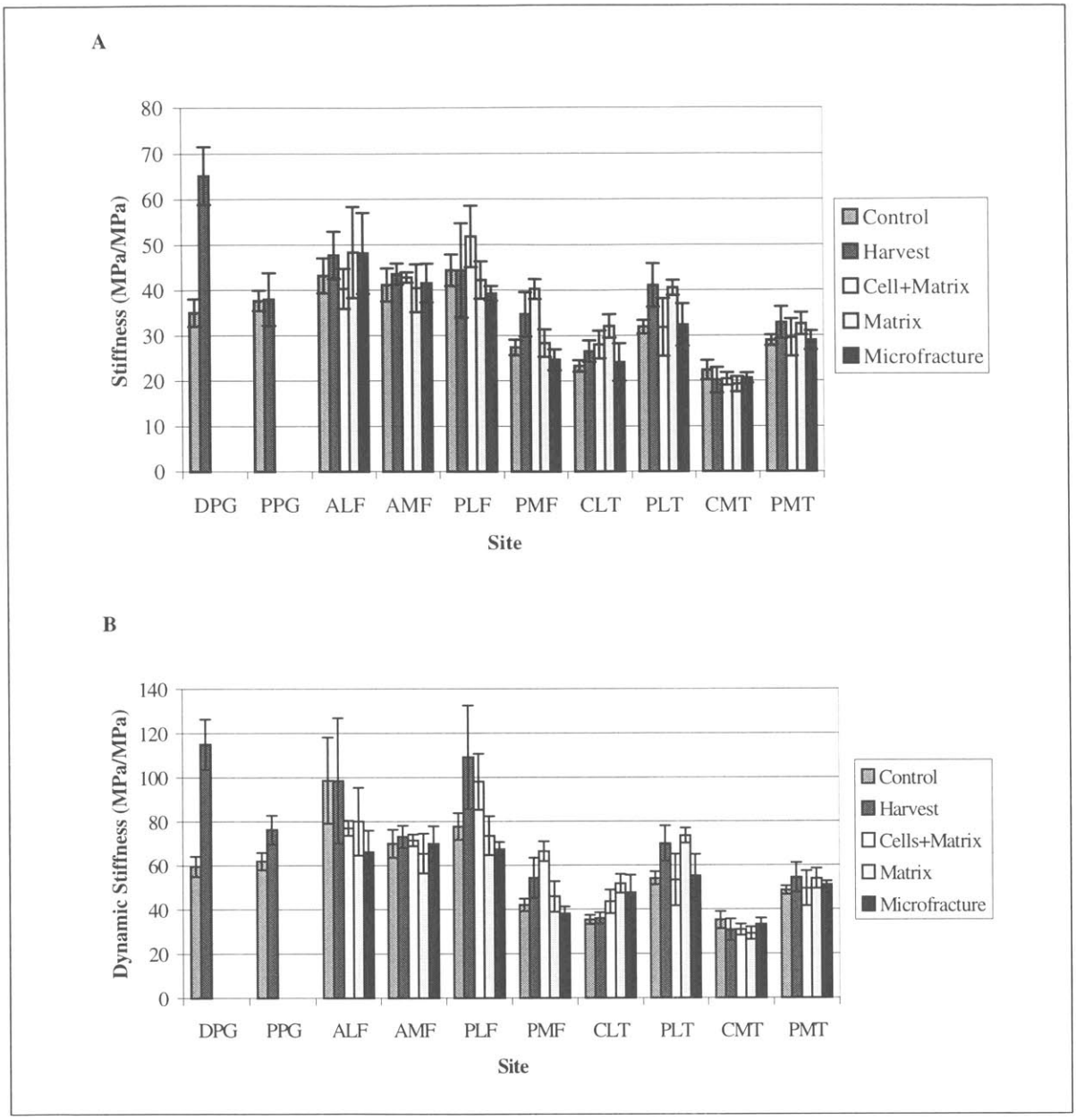

Figure 3.7 – Dynamic stiffness at **A:** 0.01 Hz and **B:** 1.0 Hz of articular cartilage at various sites in joints subjected to different surgical procedures. Values are mean ± SEM and normalized to static offset stress (n=3-7).

3.2.4 Streaming Potential

Streaming potential measurements were made at the same six frequencies as dynamic stiffness measurements. Figure 3.8 shows a typical relationship of streaming potential and frequency. Again, since differences arising at one frequency were generally seen at all frequencies, only the values at 1.0 and 0.01 Hz were normalized and analyzed in detail.

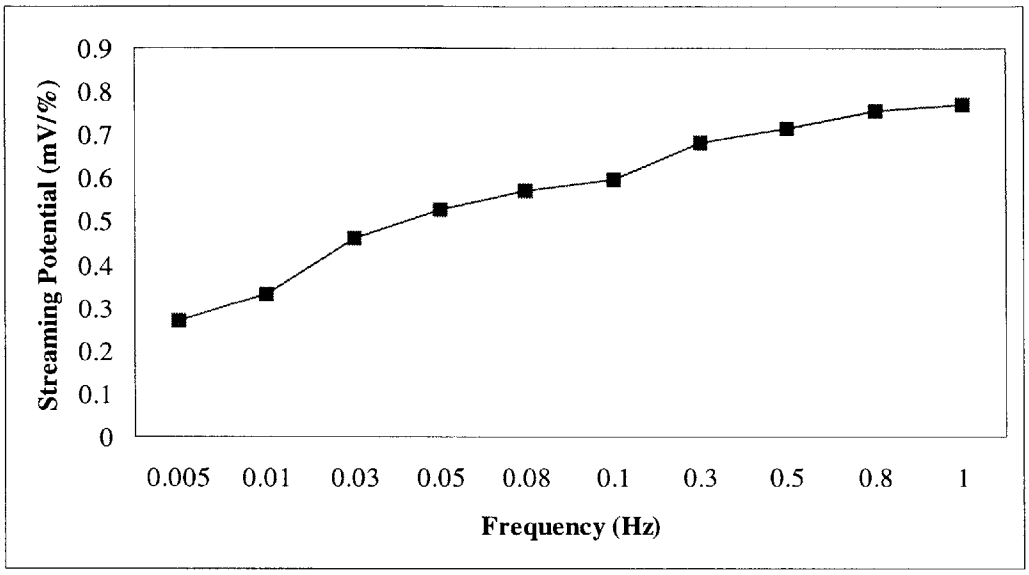

Figure 3.8 – Streaming potential versus frequency of applied displacement for a canine articular cartilage at the distal patellar groove (DPG) site in an unoperated knee.

As shown in Figure 3.9, the normalized streaming potentials of the control joints was lowest at the PPG (0.58 ± 0.17 mV/MPa at 1.0 Hz, 0.38 ± 0.08 mV/MPa at 0.01 Hz) and highest at the PLF (2.29 ± 0.20 mV/MPa at 1.0 Hz, 1.32 ± 0.11 mV/MPa at 0.01 Hz).

In terms of magnitude of change and significance of change, the largest changes between surgical groups and the control group were seen in the streaming potential measurements (Figure 3.10). Again, the direction of change for streaming potential measurements was an increase and three of the four surgical groups had at least one site demonstrating a significant change. The largest change was an increase from 0.54 ± 0.11 mV/MPa (control) to 2.17 mV/MPa at the DPG site in the harvest group ($p_{t\text{-test}}$=0.001, p_{Fisher}=0.005). Significant changes and trends are summarized as percent changes from control in Table 3.1.

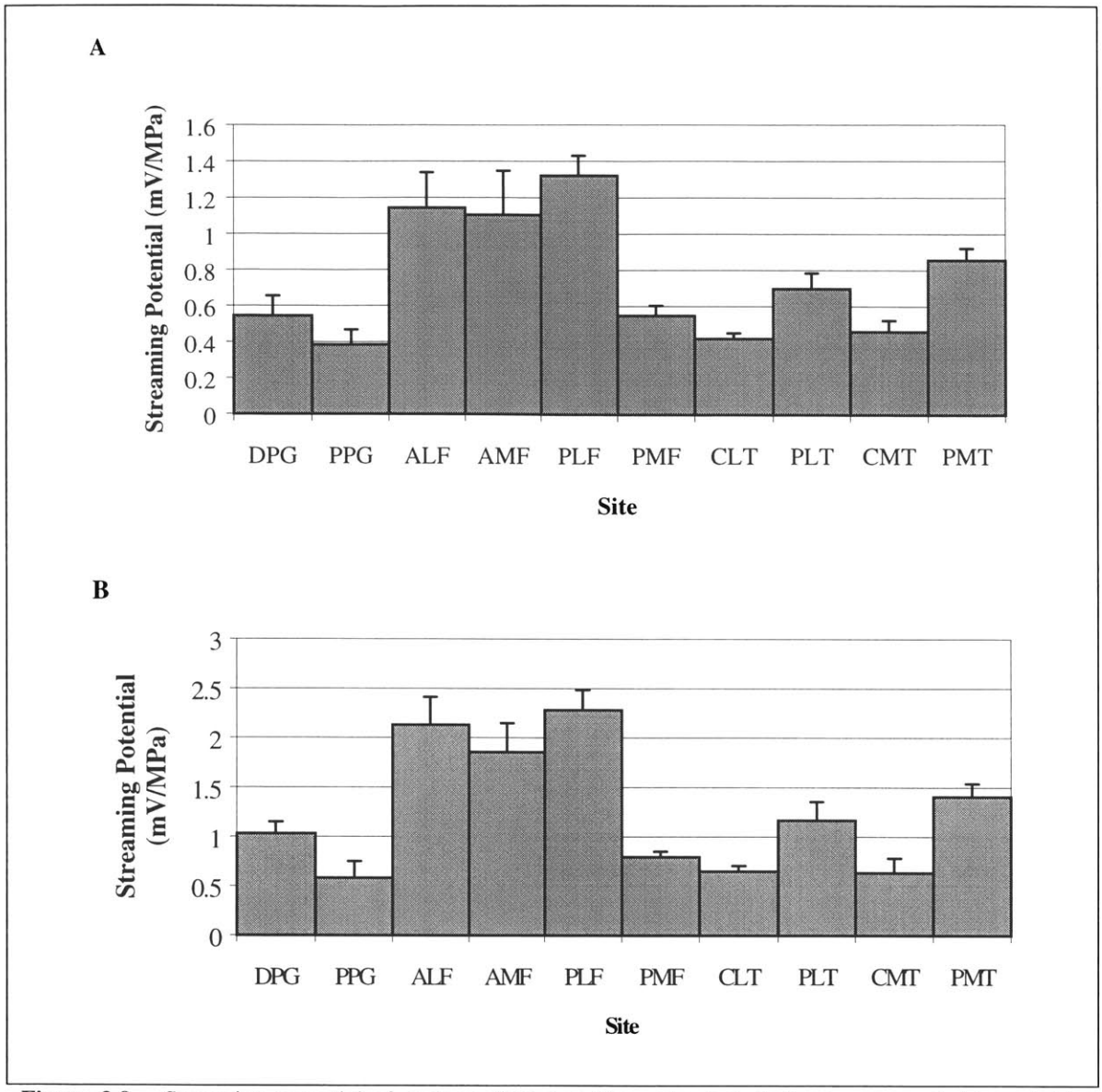

Figure 3.9 – Streaming potential of canine articular cartilage at selected sites in unoperated knee joints (n=6-7) measured at **A:** 0.01 Hz and **B:** 1.0 Hz. Values are mean ± SEM and normalized to static offset stress; n=6-7.

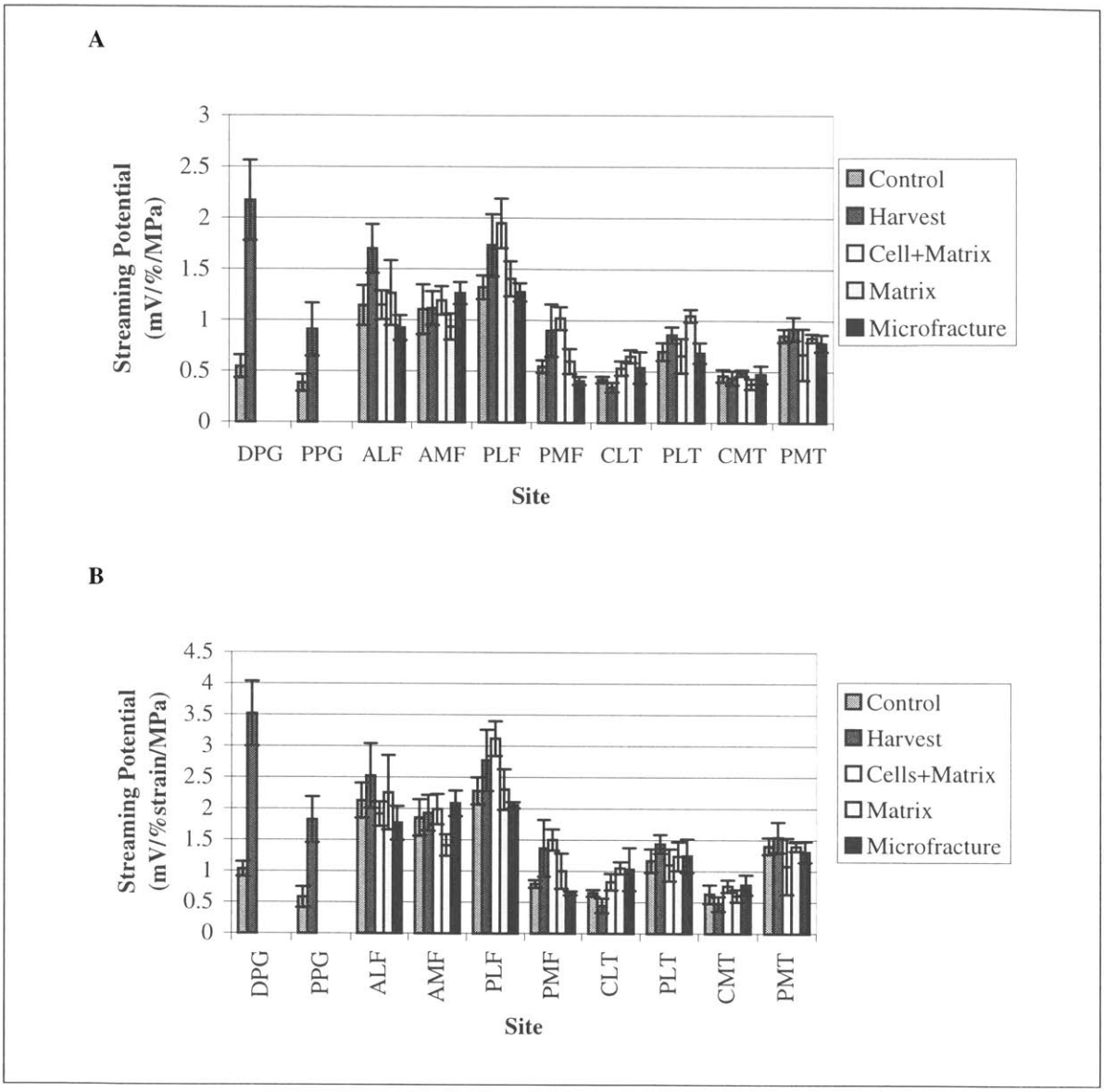

Figure 3.10– Streaming potential at **A:** 0.01 Hz and **B:** 1.0 Hz of articular cartilage at various sites in joints subjected to different surgical procedures. Values are mean ± SEM and normalized to static offset stress (n=3-7).

Table 3.1 – Changes in mechanical properties of canine knee articular cartilage following surgical procedures ($p<0.10$). Changes are shown as group/site average percent changes (± standard error of the mean) from the mean value measured at the same sites in unoperated joints. Bold-faced values indicate changes reaching a significance of $p<0.05$.

Group	Site	Thickness	Modulus	DynStf/StatStrs 0.01 Hz	DynStf/StatStrs 1.0 Hz	StrPot/StatStrs 0.01 Hz	StrPot/StatStrs 1.0 Hz
Harvest	DPG	33 ± 6		**86 ± 18**	**93 ± 19**	**299 ± 72**	**241 ± 50**
	PPG				23 ± 11	**136 ± 67**	**213 ± 63**
	PLF		-11 ± 22	32 ± 23		31 ± 23	
	PMF					64 ± 47	72 ± 57
	CLT		21 ± 41			**-17 ± 11**	**-30 ± 16**
	PLT			29 ± 15	29 ± 15		
Cell+Matrix	PLF		-25 ± 12		26 ± 16	**47 ± 18**	37 ± 11
	PMF			**47 ± 8**	**58 ± 11**	**86 ± 20**	**89 ± 21**
	CLT		**37 ± 24)**	20 ± 13	23 ± 15	27 ± 16	28 ± 20
	PMT			2 ± 14			
Matrix	PMF	-15 ± 15					
	CLT	-19 ± 9		**38 ± 11**	**46 ±12**	**54 ± 15**	**62 ± 15**
	PLT			**27 ± 5**	**36 ± 6**	**50 ± 9**	
Microfracture	PLF		-26 ± 12				
	PMF	-8 ± 7				-25 ± 7	-18 ± 4
	CLT		21 ± 41		34 ± 22		
	PMT	-19 ± 20					

3.3. Biochemical Properties

The magnitude of the change in the biochemical properties was, in general, smaller than in the mechanical properties. There were also fewer changes that reached the $p<0.05$ and $p<0.10$ levels of significance (Table 3.2).

3.3.1 Hydration

In the control joints, the PPG had the lowest water content (hydration = 2.4 ± 0.1) and the CMT had the highest water content (hydration = 4.2 ± 0.2; Figure 3.11).

There were not large variations in hydration among the different treatment groups (Figure 3.12). The only site that appeared to be significantly affected by surgical procedures was the AMF (hydration of control 2.5 ± 0.05). The harvest (2.9 ± 0.2), matrix (2.8 ± 0.1) and microfracture (2.9 ± 0.1) groups all displayed a significant ($p<0.05$) increase in hydration at this site (Table 3.2). This site in the cell-seeded matrix group also had an increased water content (2.8 ± 0.3), but the increase did not reach significance ($p_{Fisher}=0.06$).

While the femoral sites tended to show increases in hydration for the surgical groups compared to the control group, the tibial sites tended to show decreases in hydration compared to the control group (Figure 3.12). None of these changes reached significance ($p<0.05$), although some were notable. The matrix and microfracture groups showed decreases of 12.9 ± 3.8% and 16.1 ± 6.2%, respectively, at the CMT site

($p_{t\text{-}test}$=0.071 and 0.053, respectively). Additionally, the PLT site in the cell-seeded matrix group showed a decrease of 13.9 ± 6.8% (p_{Fisher}=0.088).

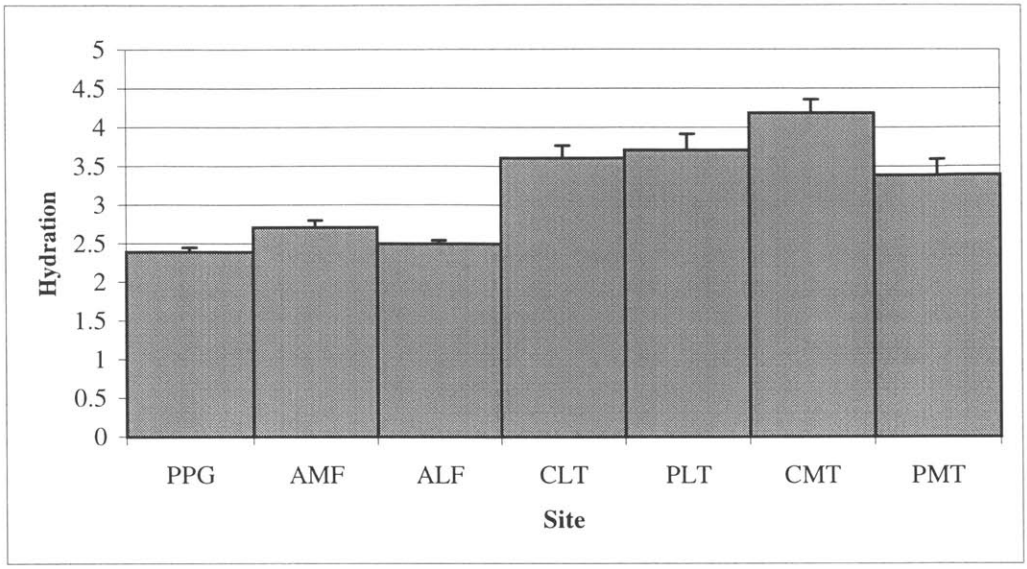

Figure 3.11 – Hydration of canine articular cartilage at selected sites in unoperated knee joints. Values are mean ± SEM, n=6-7.

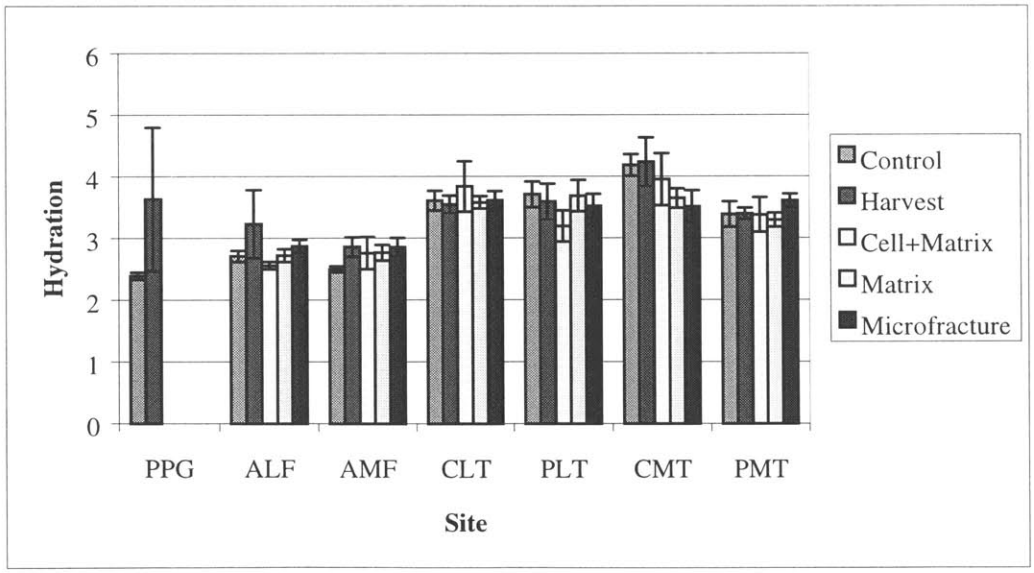

Figure 3.12 – Hydration of articular cartilage at various sites in joints subjected to different surgical procedures. Values are mean ± SEM (n=3-7).

3.3.2 Glycosaminoglycan Content

As shown in Figure 3.13, the amount of GAG per dry weight of tissue for normal articular cartilage ranged from 15.5 ± 0.8 μg/mg (ALF) to 29.0 ± 1.1 μg/mg (CMT). There were not large variations in GAG content due to surgery Figure 3.14. The PMT

was the only site that seemed to be affected by surgery. In the matrix group, the GAG content at this site increased from 16.8 ± 0.9 μg/mg to 20.8 ± 1.3 μg/mg ($p_{t\text{-}test}$=0.029, p_{Fisher}=0.024). In the harvest group, the GAG content also tended to increase (20.5 ± 1.5 μg/mg; $p_{t\text{-}test}$=0.056).

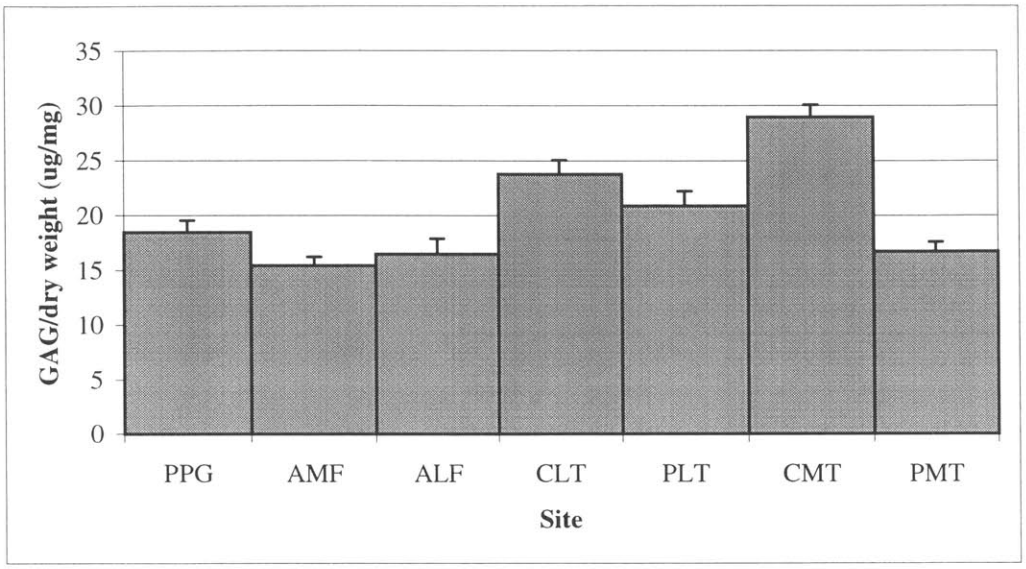

Figure 3.13 – Total GAG content of canine articular cartilage at selected sites in unoperated knee joints. Values normalized by tissue dry weight and presented as mean ± SEM, n=6-7.

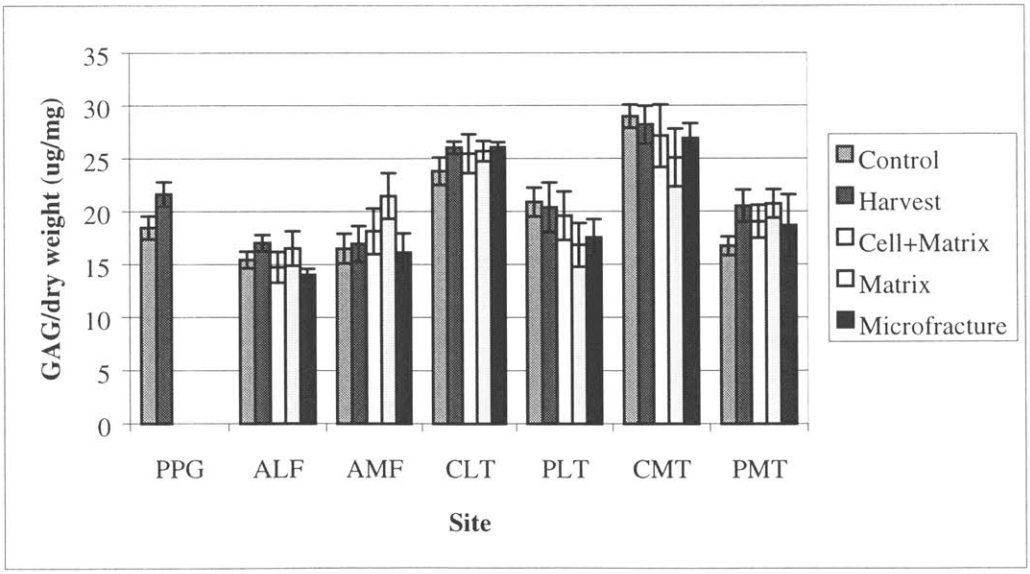

Figure 3.14 – Total GAG content of articular cartilage at various sites in joints subjected to different surgical procedures. Values are mean ± SEM (n=3-7).

3.3.3 DNA Content

The PLT site in the control group had the highest DNA content per dry weight of tissue (0.12 ± 0.008 μg/mg) and the CLT group had the lowest (0.053 ± 0.002 μg/mg) (Figure 3.15). As shown in Figure 3.16, the CMT group in the harvest and cell-seeded groups had significant increases ($p<0.05$) in DNA/dry weight. DNA content increased from 0.065 ± 0.002 μg/mg to 0.079 ± 0.004 μg/mg and 0.077 ± 0.003 μg/mg, respectively. The PMT group in the matrix group demonstrated a decrease of 22.4 ± 3.4%, but this decrease was not significant ($p_{t\text{-test}}=0.078$, $p_{Fisher}=0.088$).

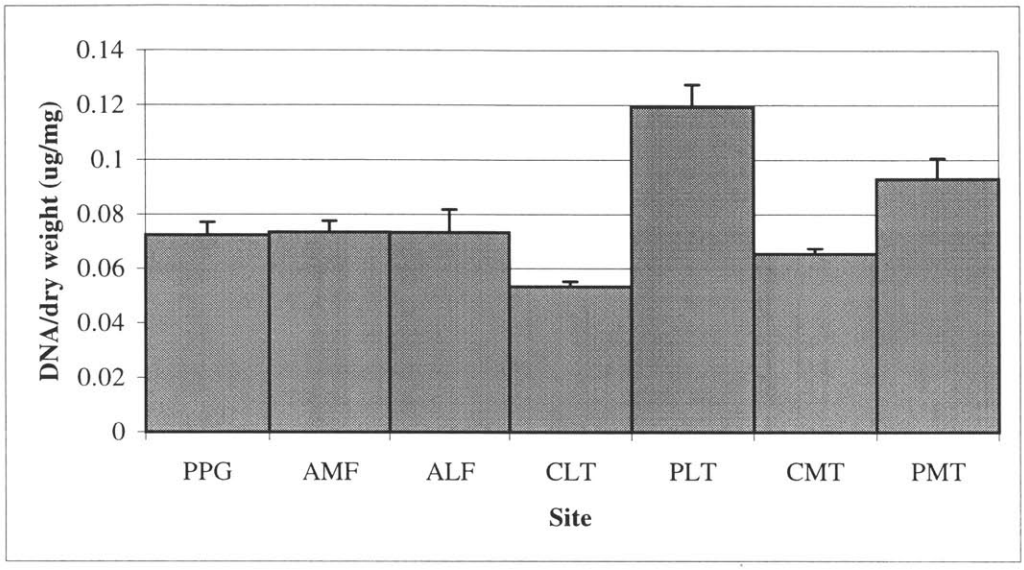

Figure 3.15 – Total DNA content of canine articular cartilage at selected sites in unoperated knee joints. Values normalized by tissue dry weight and presented as mean ± SEM, n=6-7.

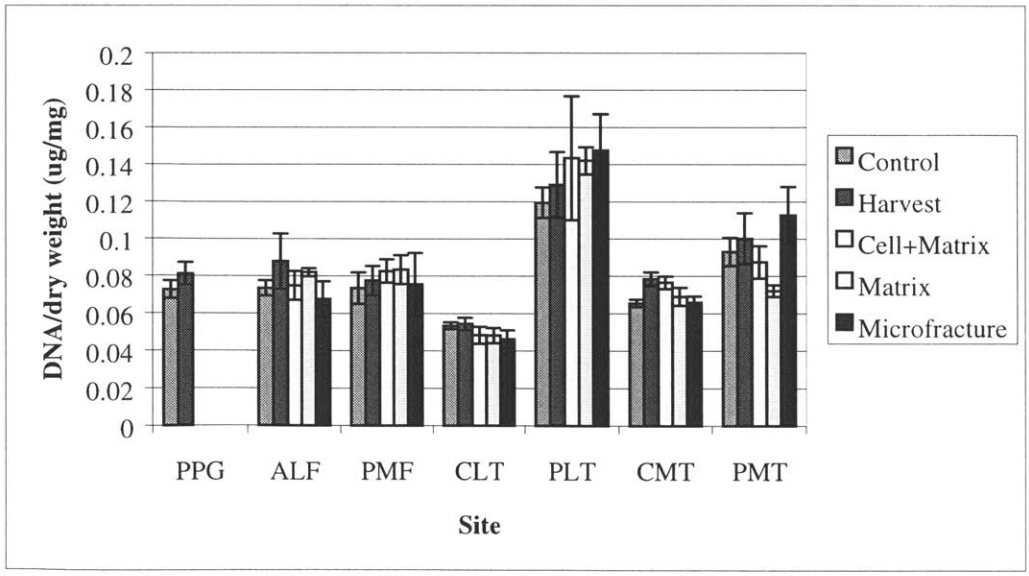

Figure 3.16 – Total DNA content of articular cartilage at various sites in joints subjected to different surgical procedures. Values are mean ± SEM (n=3-7).

Table 3.2 – Changes in biochemical composition of canine knee articular cartilage following surgical procedures ($p<0.10$). Changes are shown as group/site average percent changes (± standard error of the mean) from the mean value measured at the same sites in unoperated joints. Bold-faced values indicate changes reaching a significance of $p<0.05$.

Group	Site	Hydration	GAG/dry	DNA/dry
Harvest	AMF	**15 ± 6**		
	CMT			**20 ± 6**
	PMT		22 ± 9	
Cell+Matrix	AMF	11 ± 11		
	PLT	-14 ± 7		
	CMT			**17 ± 4**
Matrix	AMF	**11 ± 5**	30 ± 13	
	PLT			19 ± 6
	CMT	-13 ± 4		
	PMT		**24 ± 8**	-22 ± 3
Microfracture	AMF	**14 ± 6**	-2 ± 11	
	CMT	-16 ± 6		

3.4. Histology and Immunohistochemistry

3.4.1 Safranin-O Staining

DPG sections were chosen for histological analysis because this site showed the largest changes in mechanical properties. Histological sections verified that there was a difference in articular cartilage thickness between the control and harvest groups (Figure 3.17). Safranin-O sections from DPG sites were graded for osteoarthritic degeneration using the Mankin scale. All sections revealed intact bone-cartilage boundaries and had no signs of fibrillation. Safranin-O staining intensity ranged from normal to slightly decreased at the surface. Cellularity ranged from normal to slightly increased. Total scores for graded histological sections ranged from zero to two (scale 0-14 with zero being normal). No differences were seen in the scores from control and harvest groups.

3.4.2 α-Smooth Muscle Actin Staining

Immunohistochemical analysis was performed on selected specimens fixed both on the day of sacrifice and on the day of testing. The smooth muscle cells of the capillaries in the subchondral bone stained positive in both cases. Almost all of the chondrocytes in the tissue fixed on the day of sacrifice stained positive for α-smooth muscle actin. However, most of these cells appeared to have died (disrupted cytoplasm and pyknotic nuclei) prior to tissue fixation so further analysis was not performed on these tissue samples. Virtually none of the chondrocytes in the tissue fixed on the day of testing stained positive.

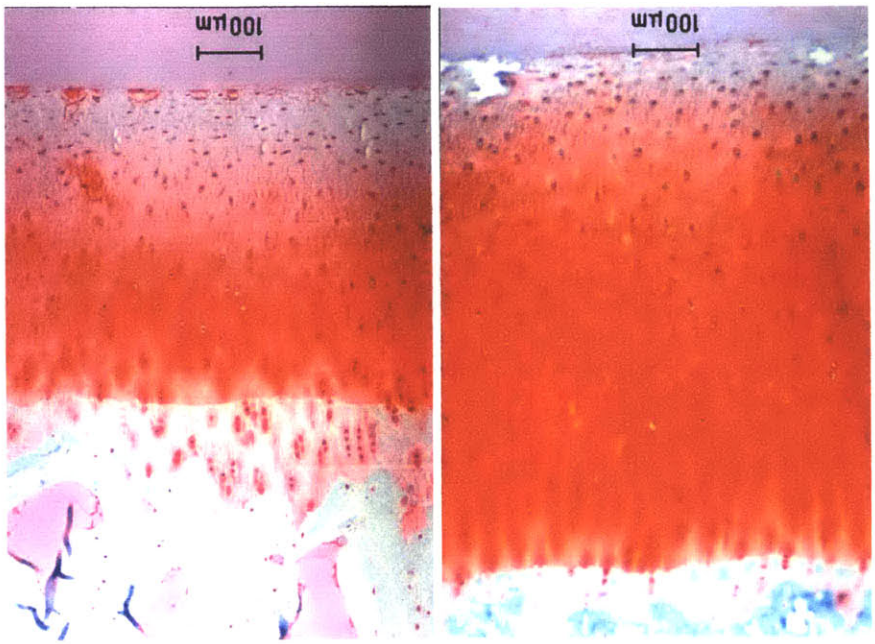

Figure 3.17 – Histological sections of canine articular cartilage from **A:** an unoperated joint and **B:** a harvest-operated joint. Both sections are graded normal (score of 0) on the Mankin scale. Specimens embedded in JB-4 and stained with Safranin-O/Fast Green.

CHAPTER 4: DISCUSSION

Although there were no obvious gross changes in the articular cartilage (*ie:* color and texture of the tissue appeared normal) distant from the defect or harvest sites of the operated joints at necropsy (fifteen to eighteen weeks post-operative), there were significant changes in some of the physical and biochemical properties of the cartilage when compared to control tissue. Figure 4.1 summarizes the sites at which changes in physical and biochemical properties were measured. These changes varied in magnitude (10-300%) and were not wide-spread. Changes in biochemical composition tended to be less frequent and of smaller magnitude (10-24%) than changes in physical properties (10-300%). The greatest changes were seen in the dynamic mechanical properties (streaming potential and dynamic stiffness) of the patellar groove sites taken from the harvest joints.

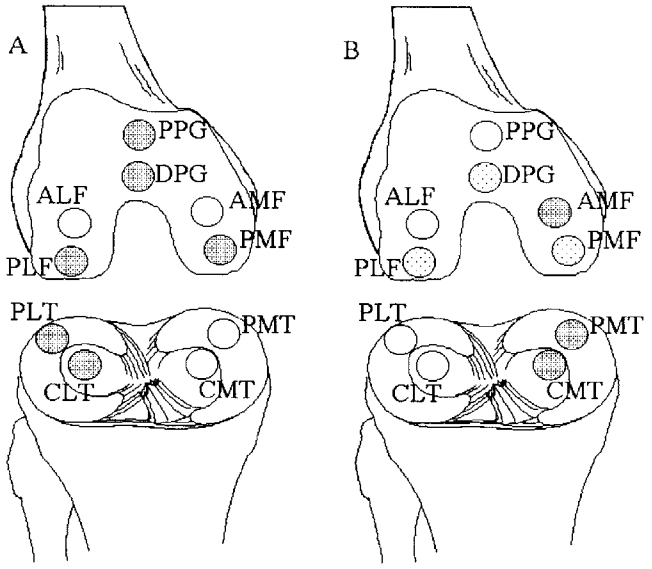

Figure 4.1 – Summary of sites (shaded) at which significant changes ($p<0.05$) in **A:** physical properties or **B:** biochemical composition were seen for at least one surgical group compared to the unoperated control group. Note that cartilage at DPG, PLF, and PMF sites was not analyzed for biochemical composition.

The healing of the articular cartilage defects was similar for all three surgical treatments (Breinan, 1998), yet the articular cartilage throughout the rest of the joint was affected differently in the different surgical groups. The fewest changes were seen in the microfracture treated group, with only one property change at one site reaching significance at $p<0.05$. The most changes (ten reaching statistical significance) were seen in the harvest group.

4.1. Comparison of Measured Values with Literature Values

The thickness and equilibrium moduli values measured for the articular cartilage from the unoperated knees were in general agreement with values found in the literature for canine articular cartilage. Reported values for thickness range from 1.0 to 1.2 mm for the tibial plateau, 0.84 to 0.87 mm for the medial condyle, 0.55 to 0.61 mm for the lateral

condyle, and 0.40 to 0.52 mm for the patellar groove (Arokoski *et al.*, 1996; Athanasiou *et al.*, 1991; Jurvelin *et al.*, 1987). A similar trend in thickness patterns was observed in this study. The cartilage was thickest at the central medial tibial plateau (1.4 ± 0.05 mm) and thinnest at the distal patellar groove (0.50 ± 0.05 mm) and thicker on the medial femoral condyle (0.72 ± 0.08 mm at AMF) than on the lateral femoral condyle (0.55 ± 0.07 mm at ALF).

Equilibrium moduli calculated in this study tended to be slightly higher than the values found in the literature although the trends are the same. The cartilage at the distal patellar groove was stiffer than other sites on the femur and the cartilage on the medial femoral condyle (2.9 ± 0.5 MPa at AMF) was stiffer than the lateral femoral condyle (1.9 ± 0.1 MPa at PLF). Literature values for Young's modulus range from 0.45 to 1.84 MPa (Athanasiou *et al.*, 1991; Hale *et al.*, 1993; Jurvelin *et al.*, 1987; Setton *et al.*, 1994). The equilibrium moduli in this study ranged from 1.9 ± 0.1 MPa at the PLF to 3.7 ± 0.7 MPa at the distal patellar groove. Although all the values obtained here were higher than most of the reported values, the modulus reported by Hale, *et al.* (1.84 MPa; Hale *et al.*, 1993) was measured by a stress relaxation test similar to the one employed in this study.

It should be emphasized that the focus of this study was on the relative changes of the articular cartilage from operated versus unoperated joints. Since the site to site trends reported in other studies were reproduced here, it seems reasonable that the relative changes seen between surgical groups and the control group are valid.

Additionally, it should be emphasized that previous studies have found that there are no differences between articular cartilage from the right and left knee joints (Athanasiou *et al.*, 1991). This allows the comparison of properties measured in surgically treated (right) knees with those measured in unoperated (left) knees.

4.2. Statistical Validation

There was a wide range in the coefficient of variation for the various mechanical and biochemical parameters. For the large majority of variables, however, the coefficient of variation was under 0.5. Although the standard deviation for many cases exceeded the 20% estimation used in the power calculation, the changes in certain properties were also much greater than the 50% change used in the calculation.

Fisher's exact test was used in addition to the Student's t-test because it is less affected by a single outlying value when the sample sizes are small. However, for the majority of the parameters, if significance ($p<0.05$) was seen by either the Student's t-test or the Fisher exact test, it was seen by both statistical tests.

4.3. Correlation of Physical and Biochemical Property Changes

Correlations between changes in physical properties and biochemical composition have been extensively reported (Altman *et al.*, 1984; Armstrong and Mow, 1982; Buckwalter and Mankin, 1998; Guilak *et al.*, 1994; Hoch *et al.*, 1983; Setton *et al.*, 1993). For instance, increases in water content have been associated with decreases in tensile (Guilak *et al.*, 1994) and compressive equilibrium (Altman *et al.*, 1984; Armstrong *et al.*, 1982; Buckwalter *et al.*, 1998) and dynamic stiffnesses (Hoch *et al.*, 1983) and increases in tissue permeability (Armstrong *et al.*, 1982; Hoch *et al.*, 1983). Deviations in tissue stiffness and permeability have also been linked to changes in proteoglycan content (Buckwalter *et al.*, 1998; Guilak *et al.*, 1994; Hoch *et al.*, 1983). In this study, however, changes in hydration or GAG content did not accompany changes in

stiffness (equilibrium or dynamic) and vice versa. For example, the only three sites that did not show any changes in mechanical properties (up to a significance level of $p<0.10$) were three of the five sites that did show changes ($p<0.10$) in biochemical properties. It is possible that our sample size and magnitude of change were too small to detect any correlations. It is also possible that the changes in mechanical properties at this early time point are due to tissue reorganization rather than biochemical composition and that longer-term studies would elucidate correlations between changes in biochemical make-up and mechanical properties (Setton *et al.*, 1993).

4.4. Relevance of Changes

The changes observed in this study can be summarized as predominantly increases in streaming potential and dynamic stiffness and both increases and decreases in cartilage thickness, equilibrium modulus, hydration, GAG content, and DNA content.

4.4.1 Effects of Surgery

Studies have shown that simply opening a joint can induce changes in the articular cartilage. Biochemical changes associated with arthrotomy include decreased GAG content and decreased cellular metabolism (Carney *et al.*, 1984; Speer *et al.*, 1990). The chondrocytes, however, appeared to recover within six weeks of arthrotomy. When more invasive procedures were performed, the effects were longer-lived. Sams, *et al.* (Sams *et al.*, 1995) reported a decrease in GAG content in the articular cartilage within ten millimeters of surgically created defects compared to normal cartilage four and eight months after surgery.

It is unlikely, however, that the changes seen in this study can be attributed solely to the opening of the joint or the creation of the defects. Fewer changes were seen in the microfracture-treated joints compared to other surgically treated knees. Matrices implanted alone or seeded with chondrocytes may affect the surrounding cartilage as a result of the products of matrix degradation or by agents released by the cells in response to the matrix. The additional trauma of suturing a cover over the implanted matrix may also affect the cartilage in the joint (Breinan *et al.*, 1997). In analyzing the effects of the cell-seeded matrix treatment, changes induced by the harvest procedure should also be considered, as this appeared to induce the most changes to the surrounding cartilage. Grande, *et al.*, reported that chondral defects that do not penetrate the subchondral bone appear to progress towards osteoarthritic degeneration (Grande *et al.*, 1989). The defects created by the harvest procedure are also isolated chondral defects and may also have the same potential for inducing changes in the surrounding cartilage.

4.4.2 Osteoarthritic Degeneration

Changes believed to be associated with osteoarthritis include increases in water content (Altman *et al.*, 1984; Buckwalter *et al.*, 1998; Guilak *et al.*, 1994; Mankin, 1974), and decreases in equilibrium stiffness (Guilak *et al.*, 1994; Hoch *et al.*, 1983), dynamic stiffness (Hoch *et al.*, 1983), streaming potential (Hoch *et al.*, 1983), and proteoglycan concentration (Buckwalter *et al.*, 1998; Guilak *et al.*, 1994; Hoch *et al.*, 1983; Mankin, 1974). Although there were a few cases in which the water content increased for the operated joint relative to control and, hence support the notion of degeneration, the majority of the significant changes (increases in streaming potential and dynamic stiffness) are not consistent which osteoarthritis.

4.4.3 Hypertrophic Remodeling

Prior to cartilage breakdown there is a reparative phase of hypertrophic remodeling (Brandt, 1993; Buckwalter *et al.*, 1998; Lin *et al.*, 1998). In this phase, as in the early stages of osteoarthritic degeneration, there are increases in cartilage mass and cellularity. In contrast to osteoarthritis, however, this phase is further characterized by increases in proteoglycan concentration (Brandt, 1993; Buckwalter *et al.*, 1998; Lin *et al.*, 1998) with resulting increases, not decreases, in streaming potential and dynamic stiffness (Lin *et al.*, 1998). Our observations of increased streaming potential, dynamic stiffness and DNA content are consistent with this hypertrophic remodeling.

4.5. Clinical Significance

The findings of this study should serve as a warning to clinicians and researchers investigating methods of articular cartilage repair. Selected procedures can induce changes in the cartilage of joints subjected to surgical repair of articular cartilage defects. The magnitude of the changes may depend on the invasiveness and/or complexity of the procedure. Additionally, the effects of secondary procedures, such as the harvest of autologous tissue, must be considered when analyzing the potential risk of a given repair technique. In fact, this study indicates that the harvest procedure yields the greatest change in the articular cartilage distant to the operated site.

CHAPTER 5: CONCLUSIONS

The results reported here support the hypothesis that surgical procedures can affect the physical and biochemical properties of articular cartilage distant to the treated site. These results represent changes in a canine model fifteen weeks after treatment of the defects and eighteen weeks after the harvest procedure. It is unclear how or why the changes in physical and biochemical properties develop and whether or not the changes seen in this animal model are representative of the human condition. The clinical significance is also unknown as the changes do not reflect osteoarthritic degeneration but are consistent with hypertrophic remodeling which may precede later degeneration. Nonetheless, this work highlights the need for clinicians and researchers to consider the possible risks cartilage repair procedures on the properties of the articular cartilage throughout the joint.

Additional studies are necessary to determine the time course of the observed changes. Future studies may focus on how early the alterations in mechanical and biochemical properties develop and what specific surgical procedures are more likely to lead to changes. It is also possible that certain protocols during surgery, such as flushing of the joint space with enzyme inhibitors will prevent such changes from developing. Longer-term studies are also needed to investigate if and how the changes progress. Ultimately, the importance of the findings in this thesis will be determined by whether or not the changes observed here lead to clinically meaningful problems.

REFERENCES

Altman, R. D., J. Tenenbaum, L. Latta, W. Riskin, L. N. Blanco and D. S. Howell. Biomechanical and biochemical properties of dog cartilage in experimentally induced osteoarthritis. *Ann Rheum Dis* **43**(1): 83-90, 1984.

Armstrong, C. G. and V. C. Mow. Variations in the Intrinsic Mechanical Properties of Human Articular Cartilage with Age, Degeneration, and Water Content. *J Bone Joint Surg* **64-A**(1): 88-94, 1982.

Arokoski, J. P., M. M. Hyttinen, T. Lapvetelainen, *et al.* Decreased birefringence of the superficial zone collagen network in the canine knee (stifle) articular cartilage after long distance running training, detected by quantitative polarised light microscopy. *Ann Rheum Dis* **55**(4): 253-264, 1996.

Athanasiou, K. A., M. P. Rosenwasser, J. A. Buckwalter, T. I. Malinin and V. C. Mow. Interspecies Comparisons of In Situ Intrinsic Mechanical Properties of Distal Femoral Cartilage. *J Orthop Res* **9**: 330-340, 1991.

Bird, J. L., T. Wells, D. Platt and M. T. Bayliss. IL-1 beta induces the degradation of equine articular cartilage by a mechanism that is not mediated by nitric oxide. *Biochem. Biophys Res Commun* **238**(1): 81-85, 1997.

Bonassar, L. J., E. H. Frank, J. C. Murray, *et al.* Changes in Cartilage Composition and Physical Properties due to Stromelysin Degradation. *Arthritis and Rheumatism* **38**(2): 173-183, 1995.

Brandt, K. D. Compensation and decompensation of articular cartilage in osteoarthritis. *Agents and Actions* **40**: 232-234, 1993.

Breinan, H., T. Minas, H. Hsu, S. Nehrer, C. Sledge and M. Spector. Cultured Autologous Chondrocytes Do Not Increase the Amount of Hyaline Cartilage in Chondral Defects in a Canine Model. *J Bone Joint Surg.* **79-A**(10): 1439-1451, 1997.

Breinan, H. A. Development of a Collagen-Glycosaminoglycan Analog of Extracellular Matrix to Facilitate Articular Cartilage Regeneration. *Ph.D. Thesis, Medical Engineering,* Massachusettes Institute of Technology, Cambridge, MA, 1998.

Brittberg, M., A. Lindahl, A. Nilsson, C. Ohlsson, O. Isaksson and L. Peterson. Treatment of Deep Cartilage Defects in the Knee with Autologous Chondrocyte Transplantation. *N Engl J Med* **331**(14): 889-895, 1994.

Buckwalter, J. A. and H. J. Mankin. Articular Cartilage: Degeneration and Osteoarthritis, Repair, Regeneration, and Transplantation. *AAOS Instructional Course Lectures* **47**: 487-504, 1998.

Bullough, P. G., P. S. Yawitz, L. Tafra and A. L. Boskey. Topographical variations in the morphology and biochemistry of adult canine tibial plateau articular cartilage. *J Orthop Res* **3**(1): 1-16, 1985.

Carney, S. L., M. E. J. Billingham, H. Muir and J. D. Sandy. Demonstration of increased proteoglycan turnover in cartilage explants from dogs with experimental osteoarthritis. *J Orthop Res* **2**: 201-206, 1984.

Dodge, G. R. and A. R. Poole. Immunohistochemical detection and immunochemical analysis of type II collagen degradation in human normal, rheumatoid, and osteoarthritic articular cartilages and in explants of bovine articular cartilage cultured with interleukin-1. *J Clin Invest* **83**(2): 647-661, 1989.

Frank, E. H. and A. J. Grodzinsky. Cartilage Electromechanics -- I. Electrokinetic Transduction and the Effects of Electrolyte pH and Ionic Strength. *J Biomech* **20**(6): 615-627, 1987.

Frank, E. H. and A. J. Grodzinsky. Cartilage Electromechanics -- II. A Continuum Model of Cartilage Electrokinetics and Correlation with Experiments. *J Biomech* **20**(6): 629-639, 1987.

Frank, E. H., A. J. Grodzinsky, T. J. Koob and D. R. Eyre. Streaming Potentials: A Sensitive Index of Enzymatic Degradation in Articular Cartilage. *J Orthop Res* **5**: 497-508, 1987.

Grande, D. A., M. I. Pitman, L. Peterson, D. Menche and M. Klein. The repair of experimentally produced defects in rabbit articular cartilage by autologous chondrocyte transplantation. *J Orthop Res* **7**(2): 208-218, 1989.

Guilak, F., A. Ratcliffe, N. Lane, M. P. Rosenwasser and V. C. Mow. Mechanical and biochemical changes in the superficial zone of articular cartilage in canine experimental osteoarthritis. *J Orthop Res* **12**(4): 474-484, 1994.

Hale, J. E., M. J. Rudert and T. D. Brown. Indentation Assessment of Biphasic Mechanical Property Deficits in Size-Dependent Osteochondral Defect Repair. *J Biomech* **26**(11): 1319-1325, 1993.

Havdrup, T. and H. Telhag. Scattered mitosis in adult joint cartilage after partial chondrectomy. A histological, autoradiographical and biochemical study in rabbits. *Acta Orthop Scand* **49**(5): 424-429, 1978.

Havdrup, T. and H. Telhag. Mitosis of chondrocytes in normal adult joint cartilage. *Clin Orthop* (153): 248-252, 1980.

Hayes, W. C., L. M. Keer, G. Herrmann and L. F. Mockros. A Mathematical Analysis for Indentation Tests of Articular Cartilage. *J Biomech* **5**: 541-551, 1972.

Hoch, D. H., A. J. Grodzinsky, T. J. Koob, M. L. Albert and D. R. Eyre. Early Changes in Material Properties of Rabbit Articular Cartilage After Menisectomy. *J Orthop Res* **1**: 4-12, 1983.

Imai, K., S. Ohta, T. Matsumoto, N. Fujimoto, H. Sato, M. Seiki and Y. Okada. Expression of membrane-type 1 matrix metalloproteinase and activation of progelatinase A in human osteoarthritic cartilage. *Am J Pathol* **151**(1): 245-256, 1997.

Jurvelin, J., I. Kiviranta, J. Arokoski, M. Tammi and H. J. Helminen. Indentation study of the biomechanical properties of articular cartilage in the canine knee. *Eng Med* **16**(1): 15-22, 1987.

Lee, C. and M. Spector. Status of articular cartilage tissue engineering. *Current Opinion in Orthopedics* **9**(6): 88-93, 1998.

Lin, B. Y., E. L. Sebern, E. H. Frank, *et al.* Changes in Physical and Biochemical Properties of Cartilage in the Guinea Pig Spontaneous OA Model Are Consistent with Hypertrophic Remodeling. *Trans ORS*, New Orleans, LA, 1998.

Lohmander, L. S., P. J. Neame and J. D. Sandy. The structure of aggrecan fragments in human synovial fluid. Evidence that aggrecanase mediates cartilage degradation in inflammatory joint disease, joint injury, and osteoarthritis. *Arthritis Rheum* **36**(9): 1214-1222, 1993.

Mankin, H. The reaction of articular cartilage to injury and osteoarthritis. *New Eng J Med* **291**(25): 1335-1340, 1974.

Mankin, H. J. The Response of Articular Cartilage to Mechanical Injury. *J Bone Joint Surg* **CCR**: 460-466, 1982.

Mankin, H. J., H. Dorfman, L. Lippiello and A. Zarins. Biochemical and Metabolic Abnormalities in Articular Cartilage from Osteo-Arthritic Human Hips. *J Bone Joint Surg* **53-A**(3): 523-537, 1971.

Messner, K. and J. Gillquist. Synthetic implants for the repair of osteochondral defects of the medial femoral condyle: a biomechanical and histological evaluation in the rabbit knee. *Biomaterials* **14**(7): 513-521, 1993.

Minas, T. and S. Nehrer. Current concepts in the treatment of articular cartilage defects. *Orthopedics* **20**(6): 525-538, 1997.

Nehrer, S., H. Breinan, A. Ramappa, *et al.* Canine Chondrocytes Seeded in Type I and Type II Collagen Implants Investigated In Vitro. *J Biomed Mater Res* **38**: 95-104, 1997.

Pettipher, E. R., G. A. Higgs and B. Henderson. Interleukin 1 induces leukocyte infiltration and cartilage proteoglycan degradation in the synovial joint. *Proc Natl Acad Sci U S A* **83**(22): 8749-8753, 1986.

Poole, C. A. The structure and function of articular cartilage matrices. Joint Cartilage Degradation: Basic and Clinical Aspects. J. F. Woessner, Jr. and D. S. Howell. New York, Marcel Dekker, Inc. **12:** 1-35, 1992.

Sams, A. E., R. R. Minor, J. A. M. Wootton, H. Mohammed and A. J. Nixon. Local and remote matrix responses to chondrocyte-laden collagen scaffold implantation in extensive articular cartilage defects. *Osteoarthritis Cartilage* **3**(1): 61-70, 1995.

Setton, L. A., V. C. Mow, F. J. Muller, J. C. Pita and D. S. Howell. Altered structure-function relationships for articular cartilage in human osteoarthritis and an expermental canine model. *Arthritis and Osteoarthritis* **39**: 27-48, 1993.

Setton, L. A., V. C. Mow, F. J. Muller, J. C. Pita and D. S. Howell. Mechanical properties of canine articular cartilage are significantly altered following transection of the anterior cruciate ligament. *J Orthop Res* **12**(4): 451-463, 1994.

Speer, K. P., J. J. Callaghan, A. V. Seaber and J. A. Tucker. The effects of exposure of articular cartilage to air. *J Bone Joint Surg* **72-A**(10): 1442-1450, 1990.

Testa, V., G. Capasso, M. Maffulli, A. Sgambato and P. R. Ames. Proteases and antiproteases in cartilage homeostasis. A brief review. *Clin Orthop* (308): 79-84, 1994.

Venn, M. and A. Maroudas. Chemical composition and swelling of normal and osteoarthritic femoral head cartilage. 1: Chemical composition. *Ann Rheum Dis* **36**: 121-129, 1977.

Webb, G. R., C. I. Westacott and C. J. Elson. Chondrocyte tumor necrosis factor receptors and focal loss of cartilage in osteoarthritis. *Osteoarthritis Cartilage* **5**(6): 427-437, 1997.

APPENDICES

APPENDIX A: INDENTATION TESTING PROTOCOL

A.1 Sample Preparation

1. Core 3/8" diameter osteochondral cores from desired locations (use PBS as cooling fluid) using a standard drill press fitted with a custom-made stainless steel coring bit (inner diameter 3/8").
2. Freeze cores in PBS until the day of testing
3. Thaw bone-cartilage plugs in PBE (phosphate buffered EDTA, see Appendix B)
4. Mix Quickmount, stirring until just viscous enough to pour (slightly less liquid component will lead to quicker setting without severely affecting set acrylic)
5. Spray inside of holders with WD-40 and insert cardboard circle
6. Pour Quickmount into holder, filling it 1/2–2/3 full
7. Use tweezers to hold specimen in Quickmount, making sure that cartilage surface is above Quickmount. Place specimen approximately in the center of holder, trying to get articular surface parallel to bottom of holder
8. If needed, dispense Quickmount around specimen using a syringe
9. Place PBE soaked gauze over cartilage surface
10. Wait 20-30 minutes for quickmount to completely set
11. Place mounted specimens in bath of PBE and put in 4°C refrigerator until testing (to minimize storage affects, do not store thawed for more than one test cycle prior to testing)

A.2 Dynastat Set-up

1. Insert probe and chamber, making sure to tighten collets (small wrench)
2. Attach probe electrode to amplifier (VC 1)
3. Check connections to ADC/DAC box: Lo-R displacement to ADC 0
   Load to ADC 1
   Streaming Potential Amplifier (bottom-most connection) to ADC 2
   Hi-R Displacement to ADC 3
   Streaming Potential Amplifier (VC 2) to DAC 4
   Transient to DAC 5
   DYN/EXT to Waveform
4. Calibrate load
   4.1. Use Coarse/Fine screw to get reading of 0.000
   4.2. Push in Cal button and use Gain screw to get 6.415
   4.3. Place 1 kg weight on top of load cell and use Gain screw to get 1.000
   4.4. Make sure zero suppression set at 018
5. Set B dial to 999, Dyn/Ext dial to 032. Push active button for each. Dial scale to 5.0
6. Calibrate displacement
   6.1. Switch toggle to compression
   6.2. Put displacement in Lo-R control and Hi-R read

6.3. Push in Zero button and use Hi-R Zero to get 0.000
6.4. Push in Cal button and use Hi-R Cal to get 4.945
6.5. Put displacement in Hi-R control and Lo-R read
6.6. Push in Zero button and use Lo-R Zero to get 0.000
6.7. Push in Cal button and use Lo-R Cal to get 6.692
6.8. Make sure zero suppression set at 000

7. Put displacement in Lo-R control
8. Set toggle switch to transient
9. Set servo settings: 0 1.0 5.75 5.0 8.3 7.0
10. Set filter settings as follows: High pass 0 0 0
    Low pass 1 5 6
    Multiplier off
    Roll off 0
    Mode bandpass
    Gain 20dB
    Roll off 12dB
    Multiplier 10
11. Set amplifier settings as follows: 5 mV
    Zero suppression off
    Vernier 10.0
    Cutoff low DC
    Cutoff high 10

A.3 Computer Set-up

1. From c:\cyndi run dynssp
2. Load appropriate protocol (canindent.pro)
3. Enter sample name, thickness and area (0.785 mm^2 for 1 mm indenter probe)
4. Open output file
5. Check to make sure that each control step is right
   5.1. Check Acquisition list
      5.1.1. First in list is what computer tries to control, so make sure it is displacement (not Hi-R displacement, except for thickness testing)
      5.1.2. Ramp strains should have displacement and load in list
      5.1.3. Dynamic strains should have displacement, load and potential in list
      5.1.4. Thickness should have Hi-R displacement, load and reference in list
   5.2. Check amplitude, control units (strain for stress-relaxations or mm for thickness), frequency list (dynamic only), return to baseline, max load, samples/sec
6. Check set-up and make sure that load gain is 10v/v and that all ADC/DAC connections correspond to the hook-up of the Dynastat to the computer

A.4 Testing of Samples

1. Insert sample into chamber and adjust to get centered under probe and as close to parallel as possible. Tighten all screws on chamber
2. Fill chamber with PBE and let equilibrate to swelling pressure 10 min
3. Bring load cell down until get reading of about –0.030V

4. Tighten upper collet to fix position of load cell and let equilibrate 5 min.
5. Turn on chart recorder and check set-up
   5.1. Banana plugs should be plugged in so that the tab on the side of the plug corresponds to black
   5.2. When switch on zero, the load and displacement pens should be at the right and the streaming potential pen should be in the middle
   5.3. Switch to cal
   5.4. Set chart speed to 100 mm/hr
   5.5. Set scales to green 5V, red 5V, blue 5V
6. Hit 'g' to start running the protocol
   6.1. Ramp to 10% strain (180 seconds) and hold for 320 seconds
   6.2. Ramp to 15% strain (180 seconds) and hold for 320 seconds
   6.3. Dynamic compression with amplitude of 1% strain at frequencies of 1.0, 0.5, 0.1, 0.05, 0.01, 0.005 Hz (2 cycles at each frequency)
   6.4. Ramp to 20% strain (180 seconds) and hold for 320 seconds

A.5 Thickness Measurements

1. When indentation is done, remove probe and insert needle (need to change to the smaller collet)
2. Let specimen equilibrate, unloaded in PBE for 10 min
3. Switch displacement to Hi-R control
4. Remove some of the PBE from the chamber so that the surface is not submerged
5. Submerge Ag/AgCl electrode in PBE
6. Connect needle as follows: Black alligator to metal strip on needle
   Red alligator after resistor and ADC 4
   Red plug before resistor and DAC 4
7. Chart recorder (blue, VC14) to ADC 4 (reference)
8. Reconnect chart recorder Lo-R (ADC 0) to Hi-R (ADC 3)
9. Set chart recorder scale to green 50V, red 10 V
10. Hit 'g' to run ramp protocol
    10.1. Ramp to 5 mm at rate of 2mm/second
    10.2. Electrical circuit is completed when needle probe contacts moist articular cartilage (top of cartilage)
    10.3. Step load (ideally) occurs when needle contacts subchondral bone (bottom of cartilage)

APPENDIX B: BIOCHEMICAL ASSAY PROTOCOLS

B.1 Lyophilization

Samples were lyophilized for 16-24 hours using the Labconco Freeze Dry System. Temperature set at –60°C. Vacuum pulled to at least 100 μmHg.

B.2 Papain Digestion

Lyophilized tissue was digested overnight (12-24 hours) at 60°C in a 0.125 mg/ml papain solution:

For 100 ml solution: 90 ml phosphate buffered EDTA (PBE, see below)
0.01M L-cysteine (0.176 g dissolved in 10 ml PBE and sterile filtered (0.2 μm) into 90ml PBE)
0.5 ml papain (Sigma suspension 25 mg/ml)

PBE stock solution (1L): 0.04M Na_2HPO_4 (5.68 g/L)
0.06M $NaH_2PO_4*H_2O$ (8.28 g/L)
0.01M $Na_2EDTA*2H_2O$ (3.72 g/L)
Dissolve above salts in 900 ml distilled water
Adjust pH to 6.5 with 1N HCl or 1N NaOH
Bring to volume with distilled water

B.3 GAG Assay using dimethylmethylene blue (DMMB) dye

Summary: DMMB dye binds to sulfated glycosaminoglycans and changes color from blue to purple based on concentration of GAG in solution

Equipment:

Perkin Elmer, Lambda 3B spectrophotometer
Set wavelength to 525 nm
Blank the spec with cuvette (4.5 ml polystyrene cuvette) of air

Protocol:

Run Standards (0, 62.5, 125, 250, 500, 1000, 2000 μg/ml) in triplicate
20 μl standard
2 ml DMMB dye
Blank with 0
Create standard curve (should be quadratic)
Run Samples in duplicate
20 μl sample
2 ml DMMB dye
Determine GAG concentration from standard curve

Record absorbance readings automatically on computer

GAG standards

0.02 g shark chondroitin 6-sulfate
10 ml PBE
Sterile filter (0.45 μm)
Initial concentration 2000 μg/ml
Serial dilutions in PBE: 1000, 500, 250, 125, 62.5, 0 μg/ml

DMMB dye solution (1 L)

0.016 g 1,9 dimethylmethylene blue dye
5 ml 100% ethanol
Mix in 15 ml centrifuge tube to dissolve (2-3 hours)
2.37 g NaCl
3.04 g glycine
950 ml distilled water
Add dissolved DMB to solution
Rinse tube 2x w/100% EtOH and add wash to solution
8.7 ml 1N HCl
0.2 g sodium azide (toxic!!)
pH to 3.0 with 1N HCl
Bring to volume with water
Filter solution through large filter paper
OD reading at 525 nm (4.5 ml cuvette) should be in range 0.20-0.28
Store in brown/amber bottle
Solution stable 3 months

Anything with DMMB dye is **ORGANIC WASTE!**

B.4 DNA Assay using Hoechst 33258 fluorescent dye

Summary: Bisbenzimidazole fluorescent dye Hoechst 33528 interacts with DNA dissociated from proteins of the nucleoprotein complex during standard papain digestion

Equipment:

SPF-550c, SLM Instruments Spectrafluorometer
Excitation wavelength 365 nm
Emission wavelength 458 nm
Excitation bandpass 10 nm
Emission bandpass 5 nm
Reference voltage 445
Reference gain 1
Fluorescence voltage 850
Fluorescence gain 1
Filter 3 seconds

48 mm acrylic cuvettes (#67.755 Sarstedt, Newton NC)

(for details on use of the spectrometer, *ie:* how not to burn out very expensive equipment, see protocol outlined by Andy Loening)

Protocol:

Run standards (0, 0.3125, 0.625, 1.25, 2.5, 5, 10 µg/ml) in triplicate
- 100 µl standard
- 2 ml dye
- Create standard curve (should be linear)

Run samples in duplicate
- 100 µl sample
- 2 ml dye
- Determine DNA content from standard curve

Sample/dye complex should reach equilibrium in about 15 seconds and should be stable for at least 2 hours (less than 5% decrease in fluorescence)
Record emission readings automatically on computer by hitting 'space bar'

DNA standards
- 1 mg calf thymus DNA
- 100 ml sterile PBE

Initial concentration 10 µg/ml
Serial dilutions in PBE to 5, 2.5, 1.25, 0.625, 0.3125, 0 µg/ml

DNA dye solution (0.01% Hoechst 33528 dye solution)
- 450 ml distilled water
- 50 ml 10x TEN buffer
- 50 µl Hoechst 33258 dye (10000x) (light sensitive; carcinogenic)

cover beaker in tin foil to minimize exposure to light

TEN buffer (10x)
- 100 mM Tris
- 10 mM Na_2EDTA
- 1.0 M NaCl
- pH 7.5

Anything with Hoechst dye is **ORGANIC WASTE!**

APPENDIX C: TISSUE FIXATION AND EMBEDDING PROTOCOL

C.1 Fixation

Tissue is first fixed in 10% neutral buffered formalin for 5-6 days

C.2 Decalcification

Specimens containing calcified tissue (*ie:* bone) must be decalcified for at least 28 days.

15% EDTA decalcifying solution:
For 1800 ml: 1570 ml 0.01 M PBS (Sigma #P-3813 dissolved in 1 L distilled water)
44 g NaOH
270 g Disodium Ethylenediamine Tetraacetate (EDTA) (add alternately with NaOH)
12N HCl to adjust to pH 7.4

C.3 Glycol Methacrylate (JB-4) Embedding

1. Dehydrate using program 9 on Tissue-Tek (1 hour in each alcohol 50%, 60%, 70%, 80%, 90%, 95%, 100%, 100%)
2. Infilitrate specimens twice, 2 days each, in catalyzed solution A (9g catalyst/1L solution A; JB-4 Embedding kit, Polysciences, Inc., Warrington, PA)
3. Embed in catalyzed solution A – solution B mixture (1mL solution B/25 mL catalyzed A)
4. Polymerize overnight at 4°C
5. Remove specimens from molds and store at 4°C

C.4 Paraffin Embedding

1. Dehydrate and infiltrate using program 4 on Tissue-Tek (1 hour in each alcohol 50%, 60%, 70%, 80%, 90%, 95%, 100%, 100%, 1 hour each in 2 baths of histoclear and 2 baths of paraffin)
2. Turn on freeze and heat switches on embedder
3. Embed specimens in hot paraffin
4. Allow wax to set (either on cold plate or freezer)
5. Remove from molds and store at 4°C

APPENDIX D: HISTOLOGY AND IMMUNOHISTOCHEMISTRY PROTOCOLS

D.1 Safranin-O Staining

1. Cut JB-4 blocks in 5 μm sections
2. Place slides on hot plate (setting 2) to fix section to slide
3. Stain 30 minutes in Safranin-O (0.2 g Safranin-O, 1 ml acetic acid, 100 ml distilled water)
4. Rinse with tap water
5. Counter-stain 5 minutes with Fast-Green (0.2 g Fast Green, 1 ml acetic acid, 500 ml distilled water)
6. Rinse with tap water
7. Allow to air dry
8. Coverslip with permount

D.2 Immunohistochemical Staining for α-Smooth Muscle Actin

1. Cut paraffin blocks in 7 μm sections
2. Place in oven at 50°C overnight
3. Deparaffinze and rehydrate:

xylene	2 x 30 minutes
100% EtOH	2 x 1 minute
95% EtOH	1 minute
90% EtOH	1 minute
80% EtOH	1 minute
70% EtOH	1 minute
PBS	3 minutes

4. Wipe of excess liquid and mark around samples with PAP pen (to minimize the amount of solution needed in the following steps)
5. Trypsin digestion (2-4 drops/sample of 0.01 g trypsin/10 ml PBS) for 60 minutes
6. Wash in PBS 2 x 3 minutes; wipe slides afterwards
7. Hydrogen peroxide (H_2O_2) for 5 minutes (2 drops/sample)
8. Wash in PBS 2 x 3 minutes; wipe slides afterwards
9. Block in 30% goat serum for 10 minutes
10. Incubate with primary antibody (1:400 dilution of mouse monoclonal anti-α smooth muscle actin; Sigma #A2547) or negative control (mouse serum) for 2 hours
11. Wipe slides before wash in PBS 2 x 3 minutes; wipe slides afterwards
12. Incubate with secondary antibody (2 drops/sample of 1:200 dilution of biotintylated goat anti-mouse immunoglobulin; Sigma #B7151) for 20 minutes
13. Wash in PBS 2 x 3 minutes; wipe slides afterwards
14. Quench in peroxidase (2 drops/sample of 1:50 dilution of ExtraAvidin-Conjugated Peroxidase; Sigma #E2886)
15. Wash in PBS 2 x 3 minutes; wipe slide afterwards

16. Stain with α smooth muscle actin immunohistochemical staining kit (4 ml distilled water, 1 drop 3% H_2O_2, 2 drops acetate buffer, 1 drop AEC chromagen; kit supplied by Sigma #IMMH-2) for approximately 10-15 minutes
17. Rinse in distilled water for 3 minutes
18. Counter-stain 20 minutes with Mayer's hematoxylin
19. Rinse in running tap water for 20 minutes
20. Mount with glycerol gelatin and coverslip (must be done in hood); try to avoid air bubbles
21. Let dry in hood (overnight) and store flat.

Positive staining is indicated by red or red-brown color in the cytoplasm

APPENDIX E: STATISTICS

In the statistical analysis, the hypothesis tested was that there was no difference in the mean values between groups. It was also assumed that the groups had equal variances.

E.1 Power Calculation

A power calculation was performed in order to determine the sample size that would be necessary to detect significant differences between experimental groups. The sample size can be calculated as follows:

$$n = 2(\frac{\sigma}{\delta})^2 (t_{\alpha,\nu} + t_{2\beta,\nu})$$

where: n = sample size

σ = standard deviation

δ = difference desired to detect

α = desired significance level (probability of obtaining a false positive result)

β = desired statistical power (probability of obtaining a false negative result)

$t_{\alpha,\nu}$= t statistic corresponding to a significance level α and ν degrees of freedom

$t_{2\beta,\nu}$= t statistic corresponding to a significance level 2β and ν degrees of freedom

The solutions of this equation for various σ, δ, α and β have been tabulated (Orthopedic Basic Science).

The difference (δ) between groups that would be meaningful was assumed to be a 50% change from the mean value of the controls. Based on literature values for canine articular cartilage thickness and modulus, a standard deviation (σ) of 25% was assumed. Using these values and setting the criteria for significance to be α=0.05 β=0.2 the sample size should be four.

E.2 Student's t-test

A two-tailed Student's t-test assuming equal variances and hypothesizing a difference of 0 was used to determine significance. The t-statistics and corresponding p-values were calculated using Microsoft Excel based on the following equation:

$$t = \frac{\overline{X_1} - \overline{X_2}}{\sigma_p \sqrt{1/n + 1/m}}$$

where: $\overline{X_1}, \overline{X_2}$ = sample mean

n,m = sample size

σ_p = pooled variance

$$\sigma_p^2 = \frac{(m-1)}{m+n-2} S_1^2 + \frac{(n-1)}{m+n-2} S_2^2$$

where S_1,S_2=sample variance

E.3 Fisher Exact Test

A two-tailed Fisher Exact test was also used to determine significance. The Fisher test most often used on 2x2 matrices with small m and n as follows:

	Group A	Group B	Row Total
$<a$	w	x	R_1=w+x
$>a$	y	z	R_2=y+z
Column Total	C_1=w+y	C_2=x+z	N=w+x+y+z

$$P_{crit} = \frac{(R_1!R_2!)(C_1!C_2!)}{N!(w!x!y!z!)} and$$

$$p - value = \sum (P - values \leq P_{crit})$$

Typically, for the mechanical parameters, the critical value, *a*, was at least 20% above or below the average value measured for the unoperated joints. For the biochemical parameters where the variances were smaller, *a* was at least 10% above or below the average value of the unoperated joints.